DISCLAIMER

This report was prepared as an account of work sponsored by an agency of the United States Government. Neither the United States Government nor any agency thereof, nor any of their employees, makes any warranty, express or implied, or assumes any legal liability or responsibility for the accuracy, completeness, or usefulness of any information, apparatus, product, or process disclosed, or represents that its use would not infringe privately owned rights. Reference herein to any specific commercial product, process, or service by trade name, trademark, manufacturer, or otherwise does not necessarily constitute or imply its endorsement, recommendation, or favoring by the United States Government or any agency thereof. The views and opinions of authors expressed herein do not necessarily state or reflect those of the United States Government or any agency thereof. Reference herein to any social initiative (including but not limited to Diversity, Equity, and Inclusion (DEI); Community Benefits Plans (CBP); Justice 40; etc.) is made by the Author independent of any current requirement by the United States Government and does not constitute or imply endorsement, recommendation, or support by the United States Government or any agency thereof.

SANDIA REPORT
SAND2025-07339
Printed June 2025

Sandia National Laboratories

Lightning Induced Interior Fields And Voltage Bounds For Coaxial Topologies

Larry K. Warne, Luis San Martin, and Jeffrey W. Glover

Prepared by
Sandia National Laboratories
Albuquerque, New Mexico
87185 and Livermore,
California 94550

Issued by Sandia National Laboratories, operated for the United States Department of Energy by National Technology & Engineering Solutions of Sandia, LLC.

Available to DOE and DOE contractors from
U.S. Department of Energy
Office of Scientific and Technical Information
P.O. Box 62
Oak Ridge, TN 37831

Telephone: (865) 576-8401
Facsimile: (865) 576-5728
E-Mail: reports@osti.gov
Online ordering: http://www.osti.gov/scitech

Available to the public from
U.S. Department of Commerce
National Technical Information Service
5301 Shawnee Rd
Alexandria, VA 22312

Telephone: (800) 553-6847
Facsimile: (703) 605-6900
E-Mail: orders@ntis.gov
Online order: https://classic.ntis.gov/help/order-methods/

SAND2025-07339

Unlimited Release

Printed June 2025

Lightning Induced Interior Fields & Voltage Bounds For Coaxial Topologies

L. K. Warne, Plasma/EM Software Dept.
L. San Martin, EM/Electronics Analyses Dept.
and J. W. Glover, Formerly at Sandia
Sandia National Laboratories
P. O. Box 5800
Albuquerque, NM 87185-1152

Abstract

We assemble bounding formulas for the interior fields and pin voltages inside a cylindrical coaxial Faraday cage which has been struck by lightning. Approximate formulas for penetrations through a circumferential door slot with subsequent coupling to the interior center conductor structure. Fields at the opposite open end are estimated and used to drive a capped connector and estimate interior pin voltages. Finally, penetrations through small circular holes and direct diffusion through the barrier are also addressed.

This page left blank

Contents

List of Figures

1 INTRODUCTION

This report provides approximate formulas for calculating penetrant electric and magnetic fields and resulting induced voltages inside a finite length cylindrical coaxial Faraday cage structure which has been struck by lightning. At one end a door with a circular slot causes coupling to the interior coax; reductions in coupling due to conductive door gaskets in the slot are also examined. At the other end the center conductor terminates resulting in an open-circuited coaxial arrangement. The electric field problem involves a dominant coaxial symmetric mode, but the magnetic field problem involves a dominant asymmetric coaxial mode. Our purpose is to determine the fields at the terminated end of the center conductor structure where a connector may be located. Approximations are given to assess the fields associated with the open circuited end of the coax and the resulting worst case pickup by a connector. Estimates for field penetrations through small circular holes and by means of direct diffusion through the cylindrical barrier are also discussed.

This page left blank

2 DOOR FIELDS

The induced voltage from a slot around the circular door at the end of the coaxial topology is derived.

2.1 Door Slot Penetration

As a worst case we assume lightning strikes the door near the circular slot, with a return on the cylinder on the opposite side of the slot. The return can be through a breakdown which is taken to occur 180 degrees around the slot at some gasket defect, or the return is at a door hinge. The current then flows in the walls of the slot with the distribution (where the azimuth coordinate is $s = b\varphi$)

$$I(s,t) = \pm\frac{1}{2}I_0(t) = \frac{1}{2}I_0(t)\,\mathrm{sgn}(s) \;\;,\;\; -h < s < h \tag{1}$$

$$2h = 2\pi b \tag{2}$$

where b is the approximate cylinder radius. The slot external inductance per unit length is [1]

$$1/L = 1/L^{intr} + 1/L^{extr} \tag{3}$$

where the interior part is ($\mu_0 = 4\pi \times 10^{-7}$ H/m is the magnetic permeability of free space)

$$L^{intr} = \mu_0 w/d \tag{4}$$

and the exterior part is

$$L^{extr} \sim \pi\mu_0/\Omega_e^{extr} \tag{5}$$

with

$$\Omega_e^{extr} = 2\ln\left(2h/a_e^0\right) + C_e \tag{6}$$

$$C_e = 2\left(\ln 2 - 7/3\right) \tag{7}$$

$$a_e^0 \sim \frac{2w}{\pi e} \;,\; d > 0.3w \tag{8}$$

The transmission line equation for the slot voltage is

$$\frac{d}{ds}V(s,t) = -L\frac{\partial}{\partial t}I(s,t) \tag{9}$$

where

$$V(\pm h,t) \approx 0 \tag{10}$$

The integration then gives

$$V(s,t) = \frac{1}{2}\left(h - |s|\right)L\frac{\partial}{\partial t}I_0(t) \tag{11}$$

The average external door voltage used to drive the symmetric (in azimuth) coaxial problem, is then

$$\langle V_{ext}\rangle = \frac{1}{2h}\int_{-h}^{h} V(s,t)\,ds = \frac{1}{2h}L\frac{\partial}{\partial t}I_0(t)\int_0^h (h-s)\,ds = \frac{1}{4}hL\frac{\partial}{\partial t}I_0(t) \tag{12}$$

Note that for large slot depth compared to the slot width $d >> w$, we can approximate and bound the total inductance per unit length L by the interior part L^{intr}

$$V(s,t) \lesssim \frac{1}{2}(h-|s|) L^{intr} \frac{\partial}{\partial t} I_0(t) \tag{13}$$

and average door voltage

$$\langle V_{ext}(t) \rangle \lesssim \frac{1}{4} h L^{intr} \frac{\partial}{\partial t} I_0(t) \tag{14}$$

2.2 Finitely Conducting Slot Walls

When the metallic slot walls are finitely conducting with conductivity σ and magnetic permeability μ, there is a surface electric field present, which is related to the surface magnetic field through [1], [2]

$$E_0(t) = \sqrt{\mu/\sigma} \frac{\partial^{1/2}}{\partial t^{1/2}} H_0(t) \tag{15}$$

For a linear ramp magnetic field in time (with rise time τ_r) this becomes [1]

$$H_0(t) = H_0(t/\tau_r) \ , \ 0 < t < \tau_r \tag{16}$$

$$E_0(t) = (H_0/\tau_r) \sqrt{\frac{4\mu t}{\pi\sigma}} \tag{17}$$

We approximate the interior slot surface magnetic field by the total slot current divided by the slot depth

$$H(s,t) \lesssim I(s,t)/d = \mathrm{sgn}(s) I_0(t) / (2d) \tag{18}$$

The internal slot voltage is then (one half the contribution results from each of the parallel interior walls)

$$\frac{1}{2} V_{int}(s,t) \lesssim \frac{1}{2}(h-|s|) \frac{1}{d} \sqrt{\mu/\sigma} \frac{\partial^{1/2}}{\partial t^{1/2}} I_0(t) \tag{19}$$

For a linear ramp current in time

$$I_0(t) = I_0(t/\tau_r) \ , \ 0 < t < \tau_r \tag{20}$$

$$\frac{1}{2} V_{int}(s,t) \lesssim \frac{1}{2}(h-|s|) \frac{1}{d} \sqrt{\mu/\sigma} (I_0/\tau_r) \sqrt{\frac{4\mu t}{\pi\sigma}} \tag{21}$$

The average is then

$$\langle V_{int}(t) \rangle \lesssim \frac{1}{2} h \frac{1}{d} \sqrt{\mu/\sigma} \frac{\partial^{1/2}}{\partial t^{1/2}} I_0(t) \tag{22}$$

and for the ramp current profile

$$\langle V_{int} \rangle \lesssim \frac{1}{2} h \frac{1}{d} (I_0/\tau_r) \sqrt{\frac{4\mu t}{\pi\sigma}} \tag{23}$$

The total average is then

$$\langle V_{tot}(t)\rangle = \langle V_{ext}(t)\rangle + \langle V_{int}(t)\rangle \lesssim \frac{1}{4}hL^{intr}\frac{\partial}{\partial t}I_0(t) + \frac{1}{2}h\frac{1}{d}\sqrt{\mu/\sigma}\frac{\partial^{1/2}}{\partial t^{1/2}}I_0(t) \tag{24}$$

and for the ramp current profile

$$\langle V_{tot}\rangle = \langle V_{ext}\rangle + \langle V_{int}\rangle \lesssim \frac{1}{4}hL^{intr}(I_0/\tau_r) + \frac{1}{2}h\frac{1}{d}(I_0/\tau_r)\sqrt{\frac{4\mu t}{\pi\sigma}} = \frac{1}{4}\frac{h}{d}\left(\mu_0 w + 2\sqrt{\frac{4\mu t}{\pi\sigma}}\right)(I_0/\tau_r) \tag{25}$$

To obtain an approximation for the largest value of the voltage we can set $t = \tau_r$

$$\langle V_{tot}\rangle \lesssim \frac{1}{4}\frac{h}{d}\left(\mu_0 w + 2\sqrt{\frac{4\mu\tau_r}{\pi\sigma}}\right)(I_0/\tau_r) = \frac{\pi b}{4d}\left(w + \frac{2}{\mu_0}\sqrt{\frac{4\mu\tau_r}{\pi\sigma}}\right)\mu_0(I_0/\tau_r) \tag{26}$$

For one-percentile worst case lightning we can take $I_0 = 200$ kA and $\tau_r = 0.5$ μs. If we have stainless steel slot walls $\sigma = 1.4 \times 10^6$ S/m, $\mu = \mu_0$ and

$$\frac{2}{\mu_0}\sqrt{\frac{4\mu\tau_r}{\pi\sigma}} \approx 1.2031 \text{ mm} \tag{27}$$

For commercial aluminum slot walls $\sigma = 2.6 \times 10^7$ S/m, $\mu = \mu_0$ and

$$\frac{2}{\mu_0}\sqrt{\frac{4\mu\tau_r}{\pi\sigma}} \approx 0.2792 \text{ mm} \tag{28}$$

2.3 Hinge Inductance

Hinges (and/or latches) on the circular door often have a high inductance so they are sometimes ignored versus a breakdown (however, the rise rate is increased in a breakdown event due to the shorter voltage collapse time). The hinge inductance model can be approximated by a half loop or a half solenoid, depending on the hinge (azimuthal) length. A half loop of radius R_{loop} and wire radius a_{loop} on a ground plane has inductance

$$L_{halfloop} = \frac{1}{2}\mu_0 R_{loop}\left[\ln\left(8R_{loop}/a_{loop}\right) - 2\right] \tag{29}$$

A half single-turn solenoid of radius R_{hinge} and length ℓ_{hinge} on a ground plane is

$$L_{halfsol} = \frac{1}{2}\mu_0\pi R_{hinge}^2/\ell_{hinge} \tag{30}$$

A correction to the solenoid is [3]

$$L_{hinge} = L_{halfsol} = \frac{1}{2}\mu_0\pi R_{hinge}^2/\left(\ell_{hinge} + 0.9R_{hinge}\right)\ ,\ \ell_{hinge} > 0.8R_{hinge} \tag{31}$$

For some hinge designs we can add two quarter loop inductances (each one half the half loop inductance) in parallel at the ends of the half solenoid geometry to complete the connection to the door. In this case the total hinge inductance is taken as

$$L_{hinge} = L_{halfsol} + \frac{1}{2}\cdot\frac{1}{2}L_{halfloop} \tag{32}$$

The voltage across the hinge is then

$$V_{hinge} = L_{hinge} \frac{\partial}{\partial t} I_0(t) \tag{33}$$

We could add the internal impedance contribution, but since this hinge inductance is usually substantial we neglect internal impedance. This terminating hinge voltage is added to the slot voltage distribution. For a linear ramp current in time

$$I_0(t) = I_0(t/\tau_r) \ , \ 0 < t < \tau_r \tag{34}$$

$$V_{hinge} = L_{hinge}(I_0/\tau_r) \tag{35}$$

The total voltage across the door-to-cylinder then consists of the sum of this constant hinge voltage and the slot voltage.

2.4 Conductive Slot Gasket

We now consider a conductive gasket occupying a depth $d_g < d$ in the door slot. We bound the penetration in this section by assuming that the decay length in the gasket is larger than the gasket depth d_g.

2.4.1 Gasket Decay Length

The decay length in the gasket is approximated by the skin depth in the gasket material, with electrical conductivity σ_g and magnetic permeability μ_g

$$\delta_g = \sqrt{2/(\omega \mu_g \sigma_g)} \approx \sqrt{2\tau_r/(\mu_g \sigma_g)} \tag{36}$$

which is assumed to be larger than the gasket depth d_g (if this is not true there will also be exponential decay in the gasket depth direction).

2.4.2 Time Domain Conductive Gasket Voltage

The slot transmission line equations in this case are

$$\frac{\partial V}{\partial s} = -L \frac{\partial I}{\partial t} \tag{37}$$

$$\frac{\partial I}{\partial s} = -GV \tag{38}$$

where we take the gasket conductance per unit length to be

$$G = \sigma_g d_g / w \tag{39}$$

and assuming the gasket permeability is that of free space $\mu_g \to \mu_0$, we can approximate the inductance per unit length as

$$L \leq L^{intr} = \mu_0 w/d \tag{40}$$

Eliminating the slot voltage gives

$$\frac{\partial^2 I}{\partial s^2} = LG \frac{\partial I}{\partial t} \tag{41}$$

To find solutions we first let

$$I = t^{\beta} F(\xi) \ , \ \xi = s/t^{\alpha} \tag{42}$$

Substituting into the partial differential equation yields

$$t^{1-2\alpha} \frac{d^2}{d\xi^2} F(\xi) = LG \left[\beta F(\xi) - \alpha \xi \frac{d}{d\xi} F(\xi) \right] \tag{43}$$

Choosing $\alpha = 1/2$ to eliminate the explicit t dependence, and for convenience letting $\xi = 2u/\sqrt{LG}$, gives the ordinary differential equation

$$\frac{d^2}{du^2} F(u) + 2u \frac{d}{du} F(u) - 4\beta F(u) = 0 \tag{44}$$

The solutions are the iterated complementary error functions [4]

$$F(u) = A i^{2\beta} \mathrm{erfc}(u) + B i^{2\beta} \mathrm{erfc}(-u) \tag{45}$$

where

$$i^n \mathrm{erfc}(u) = \int_u^{\infty} i^{n-1} \mathrm{erfc}(u') \, du' \tag{46}$$

$$i^0 = \mathrm{erfc}(u) \tag{47}$$

$$i^{-1} \mathrm{erfc}(u) = \frac{2}{\sqrt{\pi}} e^{-u^2} \tag{48}$$

$$i^1 \mathrm{erfc}(u) = -u \mathrm{erfc}(u) + \frac{1}{\sqrt{\pi}} e^{-u^2} \tag{49}$$

$$i^2 \mathrm{erfc}(u) = \frac{1}{2} \left(\frac{1}{2} + u^2 \right) \mathrm{erfc}(u) - \frac{u}{2} \frac{1}{\sqrt{\pi}} e^{-u^2} \tag{50}$$

$$i^3 \mathrm{erfc}(u) = -\frac{u}{3} \left[\frac{1}{2} \left(\frac{3}{2} + u^2 \right) \mathrm{erfc}(u) - \frac{u}{2} \frac{1}{\sqrt{\pi}} e^{-u^2} \right] + \frac{1}{6\sqrt{\pi}} e^{-u^2} \tag{51}$$

$$i^4 \mathrm{erfc}(u) = -\frac{u}{4} \left[-\frac{u}{3} \left[\frac{1}{2} \left(\frac{3}{2} + u^2 \right) \mathrm{erfc}(u) - \frac{u}{2} \frac{1}{\sqrt{\pi}} e^{-u^2} \right] + \frac{1}{6\sqrt{\pi}} e^{-u^2} \right] + \frac{1}{8} \left[\frac{1}{2} \left(\frac{1}{2} + u^2 \right) \mathrm{erfc}(u) - \frac{u}{2} \frac{1}{\sqrt{\pi}} e^{-u^2} \right]$$

Note that

$$\lim_{u \to 0} i^n \mathrm{erfc}(u) = \frac{1}{2^n \Gamma(n/2 + 1)} \tag{52}$$

$$\lim_{u \to 0} i^2 \mathrm{erfc}(u) = 1/4 \tag{53}$$

Choosing $\beta = 1$ for a linear ramp current in time at $s = 0$, and selecting $B = 0$ for vanishing value at $u \to \infty$

$$F(u) = A i^2 \mathrm{erfc}(u) \tag{54}$$

with

$$\frac{1}{2}s\sqrt{LG/t}=u \tag{55}$$

we have current distribution

$$I\left(s,t\right)=Ati^{2}\mathrm{erfc}\left(u\right)=At\left[\frac{1}{2}\left(\frac{1}{2}+\frac{1}{4}s^{2}LG/t\right)\mathrm{erfc}\left(\frac{1}{2}s\sqrt{LG/t}\right)-\frac{1}{4}s\sqrt{LG/t}\frac{1}{\sqrt{\pi}}e^{-\frac{1}{4}s^{2}LG/t}\right] \tag{56}$$

where the constant A is determined from I_0 by means of

$$I\left(0,t\right)=At/4=\frac{1}{2}\left(I_{0}/\tau_{r}\right)t \tag{57}$$

The derivative is

$$\frac{\partial}{\partial s}I\left(s,t\right)=At\frac{\partial u}{\partial s}\frac{\partial}{\partial u}i^{2}\mathrm{erfc}\left(u\right)=-A\frac{1}{2}\sqrt{LGt}i^{1}\mathrm{erfc}\left(u\right)=A\frac{1}{2}\sqrt{LGt}\left[u\mathrm{erfc}\left(u\right)-\frac{1}{\sqrt{\pi}}e^{-u^{2}}\right] \tag{58}$$

$$\frac{\partial I}{\partial s}\left(0,t\right)=-A\frac{1}{2}\sqrt{LGt/\pi} \tag{59}$$

Thus the voltage is

$$V\left(s,t\right)=-\frac{1}{G}\frac{\partial}{\partial s}I\left(s,t\right) \tag{60}$$

with value at $s=0$

$$V\left(0,t\right)=-\frac{1}{G}\frac{\partial I}{\partial s}\left(0,t\right)=A\frac{1}{2}\sqrt{\frac{Lt}{\pi G}}=\left(I_{0}/\tau_{r}\right)\sqrt{\frac{Lt}{\pi G}} \tag{61}$$

Taking the maximum of the voltage at the rise time (after which the current changes from the linear ramp)

$$V\left(0,\tau_{r}\right)=\left(I_{0}/\tau_{r}\right)\sqrt{\frac{L\tau_{r}}{\pi G}} \tag{62}$$

These distributions of voltage and current apply to the finite length slot provided the decay length is smaller than the slot half length $h=\pi b$.

The average voltage around the slot is then

$$\left\langle V\left(s,t\right)\right\rangle =\frac{1}{\pi b}\int_{0}^{\pi b}V\left(s,t\right)ds=\frac{1}{\pi bG}\left[I\left(0,t\right)-I\left(\pi b,t\right)\right]=\frac{I\left(0,t\right)}{\pi bG}=\frac{1}{2\pi bG}\left(I_{0}/\tau_{r}\right)t \tag{63}$$

Taking the maximum at $t=\tau_r$

$$\left\langle V\left(s,\tau_{r}\right)\right\rangle =\frac{I_{0}}{2\pi bG}=\frac{wI_{0}}{2\pi b\sigma_{g}d_{g}} \tag{64}$$

For very conductive gaskets these voltages are typically much smaller than the case without a very conductive gasket.

$$\left\langle V\left(s,\tau_{r}\right)\right\rangle /\left\langle V_{ext}\right\rangle =\frac{wI_{0}}{2\pi b\sigma_{g}d_{g}}/\left[\frac{1}{4}hL\left(I_{0}/\tau_{r}\right)\right]=\frac{2\left(d/d_{g}\right)}{\left(\pi b\right)^{2}\sigma_{g}\left(\mu_{0}/\tau_{r}\right)} \tag{65}$$

2.4.3 Conductive Gasket With Gap

If there is a small gap $2h_{gap}$ in the conductive gasket length dimension, there will be an inductive voltage contribution from the gap in addition to the preceding conductive gasket contribution. Approximating this extra inductance as if the current is injected uniformly in the depth direction gives the extra leading term (ignoring the internal contribution within the metal)

$$V_{tot} = Lh_{gap}\frac{1}{2}\left(I_0/\tau_r\right) + V\left(0,\tau_r\right) = \mu_0\frac{w}{d}h_{gap}\frac{1}{2}\left(I_0/\tau_r\right) + V\left(0,\tau_r\right) \tag{66}$$

If this gap is small in azimuth its average over azimuth will be relatively small

$$\langle V_{tot}\rangle \approx \frac{1}{2}\frac{h_{gap}}{\pi b}Lh_{gap}\frac{1}{2}\left(I_0/\tau_r\right) + \langle V\left(s,t\right)\rangle = \frac{1}{2}\frac{h_{gap}}{\pi b}\mu_0\frac{w}{d}h_{gap}\frac{1}{2}\left(I_0/\tau_r\right) + V\left(0,\tau_r\right) \tag{67}$$

This page left blank

3 COAXIAL REGION ELECTRIC FIELD

The coaxial region has an induced field due to fields propagating in the dominant Transverse Electromagnetic Mode (TEM) mode without decay along the length, and the other higher-order modes exhibiting decay. We first estimate the electric field at the end of the terminated center (inner) conductor. We next estimate the capacitance element between the door and the center conductor near the door; this is used to estimate the induced center conductor voltage from the door excitation voltage.

3.1 Fields In Coaxial And Cylindrical Regions

Taking the electric displacement $\underline{D}$ and electric field $\underline{E}$ to be determined from the electric vector potential $\underline{A}_e$ by means of

$$\underline{D} = \varepsilon_0 \underline{E} = -\nabla \times \underline{A}_e \tag{68}$$

where Faraday's law in this low frequency limit is

$$\nabla \times \underline{E} = -\underline{J}_m \tag{69}$$

and $\underline{J}_m$ is the magnetic current density. Then substituting the potential representation gives

$$\nabla \times \nabla \times \underline{A}_e = \nabla \left(\nabla \cdot \underline{A}_e \right) - \nabla^2 \underline{A}_e = \varepsilon_0 \underline{J}_m \tag{70}$$

Using the Coulomb gauge

$$\nabla \cdot \underline{A}_e = 0 \tag{71}$$

we have

$$\nabla^2 \underline{A}_e = -\varepsilon_0 \underline{J}_m \tag{72}$$

In this case we take the magnetic current to be φ-directed and to be independent of azimuth φ so that we only have $A_{e\varphi}$. Then using

$$\nabla^2 \underline{A}_e = \left(\nabla^2 - 1/\rho^2 \right) A_{e\varphi} \tag{73}$$

we can write

$$\left(\nabla^2 - 1/\rho^2 \right) A_{e\varphi} = \left(\frac{\partial^2}{\partial \rho^2} + \frac{1}{\rho} \frac{\partial}{\partial \rho} - \frac{1}{\rho^2} + \frac{\partial^2}{\partial z^2} \right) A_{e\varphi} = -\varepsilon_0 J_{m\varphi} \tag{74}$$

Taking the solutions to be combinations

$$A_{e\varphi} = e^{\pm \zeta_n z} R_1 \left(\zeta_n \rho \right), \ \left(z - z_0 \right) \rho^{\pm 1} \tag{75}$$

we have the source free form

$$\left(\frac{d^2}{d\rho^2} + \frac{1}{\rho} \frac{d}{d\rho} + \zeta_n^2 - \frac{1}{\rho^2} \right) R_1 \left(\zeta_n \rho \right) = 0 \tag{76}$$

with solutions $R_1 \left(\zeta_n \rho \right)$, where

$$R_1 \left(\zeta_n \rho \right) = J_1 \left(\zeta_n \rho \right), Y_1 \left(\zeta_n \rho \right) \tag{77}$$

We place the termination of the center conductor at $z = 0$ with a cylindrical problem to the right $z > 0$ and $0 < \rho < b$ and a coaxial problem to the left $z < 0$ and $a < \rho < b$.

On the right we have boundary condition

$$\left[\frac{1}{\rho}\frac{\partial}{\partial\rho}\left(\rho A_{e\varphi}\right)\right]_{\rho=b} = -\varepsilon_0 E_z\left(\rho = b\right) = 0\ ,\ z > 0 \tag{78}$$

and thus

$$A_{e\varphi} = \sum_{n=1}^{\infty} A_n^+ e^{-\xi_n z} J_1\left(\xi_n \rho\right)\ ,\ z > 0 \tag{79}$$

where only the Bessel functions can be retained due to the boundary condition and the finiteness of the solution at $\rho = 0$. Then using

$$\frac{1}{\rho}\frac{\partial}{\partial\rho}\left[\rho J_1\left(\xi_n\rho\right)\right] = \xi_n\left(\frac{\partial}{\xi_n\partial\rho} + \frac{1}{\xi_n\rho}\right) J_1\left(\xi_n\rho\right) = \xi_n J_0\left(\xi_n\rho\right) \tag{80}$$

we have radial boundary condition

$$J_0\left(\xi_n b\right) = J_0\left(j_{0,n}\right) = 0 \tag{81}$$

where

$$\xi_n = j_{0,n}/b \tag{82}$$

The Bessel function roots are [4]

$$j_{0,n} \sim \beta + \frac{1}{2\left(4\beta\right)} - \frac{31}{2\left(4\beta\right)^3 3} + \frac{3779}{3\left(4\beta\right)^5 5} + \cdots \tag{83}$$

$$\beta = \left(n - 1/4\right)\pi \tag{84}$$

$$j_{0,1} \approx 2.4048255577 \tag{85}$$

$$j_{0,2} \approx 5.5200781103 \tag{86}$$

$$j_{0,3} \approx 8.6537279129 \tag{87}$$

$$j_{0,4} \approx 11.7915344391 \tag{88}$$

$$j_{0,5} \approx 14.9309177086 \tag{89}$$

$$j_{0,6} \approx 18.0710639679 \tag{90}$$

$$j_{07} \approx 21.2116366299 \tag{91}$$

$$j_{0,8} \approx 24.3524715308 \tag{92}$$

$$j_{0,9} \approx 27.4934791320 \tag{93}$$

$$j_{0,10} \approx 30.6346064684 \tag{94}$$

On the left we have radial boundary conditions

$$\left[\frac{1}{\rho}\frac{\partial}{\partial\rho}\left(\rho A_{e\varphi}\right)\right]_{\rho=a,b} = -\varepsilon_0 E_z\left(\rho=a,b\right)=0\ ,\ z<0 \tag{95}$$

and as solution

$$A_{e\varphi} = \frac{A_0\left(z-z_0\right)}{\rho} + \sum_{n=1}^{\infty} A_n^- e^{\zeta_n z} R_1\left(\zeta_n\rho\right)\ ,\ z<0 \tag{96}$$

where

$$R_1\left(\zeta_n\rho\right) = J_0\left(\zeta_n a\right)Y_1\left(\zeta_n\rho\right) - J_1\left(\zeta_n\rho\right)Y_0\left(\zeta_n a\right) \tag{97}$$

and from

$$\frac{1}{\rho}\frac{\partial}{\partial\rho}\left[\rho R_1\left(\zeta_n\rho\right)\right] = \zeta_n\left(\frac{\partial}{\zeta_n\partial\rho}+\frac{1}{\zeta_n\rho}\right)R_1\left(\zeta_n\rho\right) = \zeta_n R_0\left(\zeta_n\rho\right) \tag{98}$$

we have

$$R_0\left(\zeta_n\rho\right) = J_0\left(\zeta_n a\right)Y_0\left(\zeta_n\rho\right) - J_0\left(\zeta_n\rho\right)Y_0\left(\zeta_n a\right) \tag{99}$$

$$R_0\left(\zeta_n a\right) = 0 \tag{100}$$

and

$$R_0\left(\zeta_n b\right) = J_0\left(\zeta_n a\right)Y_0\left(\zeta_n b\right) - J_0\left(\zeta_n b\right)Y_0\left(\zeta_n a\right) = 0 \tag{101}$$

These coaxial roots are [4]

$$\zeta_n a \sim \beta + \frac{p}{\beta} + \frac{q-p^2}{\beta^3} + \frac{r-4pq+2p^3}{\beta^5} + \cdots \tag{102}$$

$$\beta = n\pi/\left(b/a-1\right) \tag{103}$$

$$p = \frac{-1}{8b/a} \tag{104}$$

$$q = \frac{25\left(b^2/a^2+b/a+1\right)}{6\left(4b/a\right)^3} \tag{105}$$

$$r = \frac{-1073\left(b^4/a^4+b^3/a^3+b^2/a^2+b/a+1\right)}{5\left(4b/a\right)^5} \tag{106}$$

Some solutions are [4]

$$\zeta_{1,0}a \approx 2.07322886 \text{ for } a/b = 0.4 \tag{107}$$

$$\zeta_{1,0}a \approx 4.69706410 \text{ for } a/b = 0.6 \tag{108}$$

$$\zeta_{2,0}a \approx 4.17730 \text{ for } a/b = 0.4 \tag{109}$$

$$\zeta_{2,0}a \approx 9.41690 \text{ for } a/b = 0.6 \tag{110}$$

$$\zeta_{3,0}a \approx 6.27537 \text{ for } a/b = 0.4 \tag{111}$$

$$\zeta_{3,0}a \approx 14.13189 \text{ for } a/b = 0.6 \tag{112}$$

$$\zeta_{4,0}a \approx 8.37167 \text{ for } a/b = 0.4 \tag{113}$$

$$\zeta_{4,0}a \approx 18.84558 \text{ for } a/b = 0.6 \tag{114}$$

$$\zeta_{5,0}a \approx 10.46723 \text{ for } a/b = 0.4 \tag{115}$$

$$\zeta_{5,0}a \approx 23.55876 \text{ for } a/b = 0.6 \tag{116}$$

3.2 Excitation Of Modes At Junction

We next examine the excitation of modes at the junction of coaxial and cylindrical regions. If we take the radial field (or magnetic current) in the coaxial dominant mode as

$$E_\rho \approx \frac{V_0}{\rho \ln(b/a)} \ , \ a < \rho < b \ , \ z > 0 \tag{117}$$

and thus at the junction we can introduce a magnetic current density to represent the electric field

$$J_{m\varphi} = K_{m\varphi}\delta(z) = I_m \delta(z)/\rho \ , \ a < \rho < b \tag{118}$$

where the surface magnetic current density is found from the discontinuity of electric field at a surface with normal $\underline{n}$ pointing from region 1 to region 2

$$\underline{K}_m = -\underline{n} \times (\underline{E}_2 - \underline{E}_1) \tag{119}$$

We can evaluate $K_{m\varphi}(\rho)$, $I_m(\rho)$, or $E_\rho(\rho)$, as a function of ρ by expanding in a basis, with say $\rho_1 = a$ and $\rho_J = b$

$$\frac{1}{2}\rho K_{m\varphi}(\rho) = \rho E_\rho(\rho, 0) = V_0/\ln(b/a) + \sum_{j=1}^{J} E_j f_j(\rho) \tag{120}$$

A linear basis is

$$f_j(\rho) = \frac{\rho - \rho_{j-1}}{\rho_j - \rho_{j-1}} \ , \ \rho_{j-1} < \rho \leq \rho_j$$

$$= \frac{\rho_{j+1} - \rho}{\rho_{j+1} - \rho_j} \ , \ \rho_j < \rho < \rho_{j+1}$$

$$= 0 \ , \ \text{otherwise} \tag{121}$$

matching the value of $D_z = \varepsilon_0 E_z$ at $z = 0$ for $a \leq \rho = \rho_{j'} \leq b \ , \ j' = 1, ..., J$ to determine E_j values. Instead, it is advantages in carrying out the moments here to use a pulse basis

$$f_j(\rho) = 1 \ , \ \rho_{j-1/2} < \rho < \rho_{j+1/2}$$

$$= 0 \ , \ \text{otherwise} \tag{122}$$

$$\rho_j = \left(\rho_{j+1/2} + \rho_{j-1/2}\right) \tag{123}$$

The potential representations are

$$A_{e\varphi} = \frac{\varepsilon_0 V_0}{\rho \ln(b/a)} (z - z_0) + \sum_{n=1}^{\infty} A_n^- e^{\zeta_n z} R_1(\zeta_n \rho) \ , \ z < 0 \ , \ a < \rho < b \tag{124}$$

$$R_m(\zeta_n \rho) = J_0(\zeta_n a) Y_m(\zeta_n \rho) - J_m(\zeta_n \rho) Y_0(\zeta_n a) \tag{125}$$

$$A_{e\varphi} = \sum_{n=1}^{\infty} A_n^+ e^{-\xi_n z} J_1(\xi_n \rho) \ , \ z > 0 \ , \ 0 < \rho < b \tag{126}$$

Note that the z_0 term does not contribute to the fields

$$D_z = \varepsilon_0 E_z = -\frac{1}{\rho} \frac{\partial}{\partial \rho} (\rho A_{e\varphi}) \tag{127}$$

$$D_\rho = \varepsilon_0 E_\rho = \frac{\partial}{\partial z} A_{e\varphi} \tag{128}$$

We have the radial fields

$$\varepsilon_0 E_\rho = \frac{\varepsilon_0 V_0}{\rho \ln(b/a)} + \sum_{n=1}^{\infty} A_n^- \zeta_n e^{\zeta_n z} R_1(\zeta_n \rho) \ , \ z < 0 \ , \ a < \rho < b \tag{129}$$

$$\varepsilon_0 E_\rho = -\sum_{n=1}^{\infty} A_n^+ \xi_n e^{-\xi_n z} J_1(\xi_n \rho) \ , \ z > 0 \ , \ 0 < \rho < b \tag{130}$$

Orthogonality, from the section below, gives

$$\int_0^b J_1(\xi_n \rho) J_1(\xi_{n'} \rho) \rho d\rho = \frac{b^2}{2} [J_1(j_{0,n})]^2 \delta_{nn'} \tag{131}$$

$$\int_a^b R_1(\zeta_n \rho) R_1(\zeta_{n'} \rho) \rho d\rho = \frac{b^2}{2} \left[R_1^2(\zeta_n b) - \frac{4}{\pi^2 \zeta_n^2 b^2} \right] \delta_{nn'} \tag{132}$$

Applying this yields

$$\varepsilon_0 \int_a^b \left[\rho E_\rho(\rho,0) - \frac{V_0}{\ln(b/a)}\right] R_1(\zeta_n\rho)\, d\rho$$

$$= \varepsilon_0 \int_a^b \rho E_\rho(\rho,0) R_1(\zeta_n\rho)\, d\rho = -\frac{\varepsilon_0}{\zeta_n}\sum_{j=1}^{J} E_j\left[R_0\left(\zeta_n\rho_{j+1/2}\right) - R_0\left(\zeta_n\rho_{j-1/2}\right)\right]$$

$$= \sum_{n'=1}^{\infty} A_{n'}^{-}\zeta_{n'}\int_a^b R_1(\zeta_{n'}\rho) R_1(\zeta_n\rho)\,\rho d\rho = A_n^{-}\zeta_n\frac{b^2}{2}\left[R_1^2(\zeta_n b) - 4/(\pi\zeta_n b)^2\right] \tag{133}$$

$$\varepsilon_0 \int_a^b \rho E_\rho(\rho,0) J_1(\xi_n\rho)\, d\rho = \frac{\varepsilon_0 V_0}{\ln(b/a)}\left[J_0(\xi_n a)/\xi_n\right] - \frac{\varepsilon_0}{\xi_n}\sum_{j=1}^{J} E_j\left[J_0\left(\xi_n\rho_{j+1/2}\right) - J_0\left(\xi_n\rho_{j-1/2}\right)\right]$$

$$= -\sum_{n'=1}^{\infty} A_{n'}^{+}\xi_{n'}\int_a^b J_1(\xi_{n'}\rho) J_1(\xi_n\rho)\,\rho d\rho = -A_n^{+}\xi_n\frac{b^2}{2}J_1^2(j_{0,n}) \tag{134}$$

where we have used

$$\int_a^b R_1(\zeta_n\rho)\, d\rho = -\frac{1}{\zeta_n}\left[R_0(\zeta_n b) - R_0(\zeta_n a)\right] = 0 \tag{135}$$

Then we have

$$\varepsilon_0 \int_a^b \left[E_\rho(\rho,0) - \frac{V_0}{\rho\ln(b/a)}\right](\zeta_n\rho) R_1(\zeta_n\rho)\, d\rho = \varepsilon_0 \int_a^b E_\rho(\rho,0)(\zeta_n\rho) R_1(\zeta_n\rho)\, d\rho =$$

$$-\varepsilon_0\sum_{j=1}^{J} E_j\left[R_0\left(\zeta_n\rho_{j+1/2}\right) - R_0\left(\zeta_n\rho_{j-1/2}\right)\right] = \frac{1}{2}A_n^{-}\left[(\zeta_n b)^2 R_1^2(\zeta_n b) - (2/\pi)^2\right] \tag{136}$$

$$-\varepsilon_0 \int_a^b E_\rho(\rho,0)(\xi_n\rho) J_1(\xi_n\rho)\, d\rho =$$

$$-\frac{\varepsilon_0 V_0}{\ln(b/a)}J_0(\xi_n a) + \varepsilon_0\sum_{j=1}^{J} E_j\left[J_0\left(\xi_n\rho_{j+1/2}\right) - J_0\left(\xi_n\rho_{j-1/2}\right)\right] = \frac{1}{2}A_n^{+}j_{0,n}^2 J_1^2(j_{0,n}) \tag{137}$$

We next make the potential continuous at $z = 0$

$$-\frac{\varepsilon_0 V z_0}{\rho\ln(b/a)} + \sum_{n=1}^{\infty} A_n^{-} R_1(\zeta_n\rho) = \sum_{n=1}^{\infty} A_n^{+} J_1(\xi_n\rho)\ ,\ a < \rho < b \tag{138}$$

or

$$\sum_{n=1}^{\infty}\left[A_n^{+} J_1(\xi_n\rho) - A_n^{-} R_1(\zeta_n\rho)\right] = \frac{\varepsilon_0 V_0 z_0}{\rho\ln(b/a)}\ ,\ a < \rho < b \tag{139}$$

which gives the integral equation

$$\int_a^b E_\rho(\rho,0)\,G(\rho,\rho')\,d\rho$$

$$= \int_a^b E_\rho(\rho,0)\,2\sum_{n=1}^{\infty}\left[\frac{(\xi_n\rho)\,J_1(\xi_n\rho)\,J_1(\xi_n\rho')}{j_{0,n}^2 J_1^2(j_{0,n})} + \frac{(\zeta_n\rho)\,R_1(\zeta_n\rho)\,R_1(\zeta_n\rho')}{(\zeta_n b)^2 R_1^2(\zeta_n b) - (2/\pi)^2}\right]d\rho = \frac{V_0(-z_0)}{\rho'\ln(b/a)}\ ,\ a<\rho'<b \tag{140}$$

Rewriting this as

$$2\sum_{n=1}^{\infty}\left[\frac{J_1(\xi_n\rho')}{j_{0,n}^2 J_1^2(j_{0,n})}\int_a^b E_\rho(\rho,0)\,(\xi_n\rho)\,J_1(\xi_n\rho)\,d\rho\right.$$
$$\left.+\frac{R_1(\zeta_n\rho')}{(\zeta_n b)^2 R_1^2(\zeta_n b) - (2/\pi)^2}\int_a^b\left\{E_\rho(\rho,0) - \frac{V_0}{\rho\ln(b/a)}\right\}R_1(\zeta_n\rho)\,(\zeta_n\rho)\,d\rho\right]$$
$$= \frac{V_0(-z_0)}{\rho'\ln(b/a)}\ ,\ a<\rho'<b \tag{141}$$

and substituting the basis

$$\sum_{j=1}^{J}E_j\sum_{n=1}^{\infty}\left[\frac{J_1(\xi_n\rho')}{j_{0,n}^2 J_1^2(j_{0,n})}\left\{J_0\left(\xi_n\rho_{j+1/2}\right) - J_0\left(\xi_n\rho_{j-1/2}\right)\right\}\right.$$
$$\left.+\frac{R_1(\zeta_n\rho')}{(\zeta_n b)^2 R_1^2(\zeta_n b) - (2/\pi)^2}\left\{R_0\left(\zeta_n\rho_{j+1/2}\right) - R_0\left(\zeta_n\rho_{j-1/2}\right)\right\}\right]$$
$$= \frac{V_0 z_0}{2\rho'\ln(b/a)} + \frac{V_0}{\ln(b/a)}\sum_{n=1}^{\infty}\frac{J_1(\xi_n\rho')\,J_0(\xi_n a)}{j_{0,n}^2 J_1^2(j_{0,n})}\ ,\ a<\rho'<b \tag{142}$$

Applying a Galerkin scheme

$$\int_a^b f_{j'}(\rho')\,d\rho' = \int_{\rho_{j'-1/2}}^{\rho_{j'+1/2}} d\rho' \tag{143}$$

gives

$$\sum_{j=1}^{J}E'_j\sum_{n=1}^{\infty}\left[\frac{\left\{J_0\left(\xi_n\rho_{j'+1/2}\right) - J_0\left(\xi_n\rho_{j'-1/2}\right)\right\}\left\{J_0\left(\xi_n\rho_{j+1/2}\right) - J_0\left(\xi_n\rho_{j-1/2}\right)\right\}}{j_{0,n}^3 J_1^2(j_{0,n})}\right.$$
$$\left.+\frac{\left\{R_0\left(\zeta_n\rho_{j'+1/2}\right) - R_0\left(\zeta_n\rho_{j'-1/2}\right)\right\}\left\{R_0\left(\zeta_n\rho_{j+1/2}\right) - R_0\left(\zeta_n\rho_{j-1/2}\right)\right\}}{(\zeta_n b)\left\{(\zeta_n b)^2 R_1^2(\zeta_n b) - (2/\pi)^2\right\}}\right]$$

$$= \frac{1}{2}(-z_0/b)\ln\left(\rho_{j'+1/2}/\rho_{j'-1/2}\right) + \sum_{n=1}^{\infty}\frac{\left\{J_0\left(\xi_n\rho_{j'+1/2}\right) - J_0\left(\xi_n\rho_{j'-1/2}\right)\right\}J_0(\xi_n a)}{j_{0,n}^3 J_1^2(j_{0,n})}\ ,\ j'=1,...J \tag{144}$$

where we have set

$$E_j = \frac{V_0}{\ln(b/a)} E'_j \tag{145}$$

and

$$\frac{1}{2}\rho K_{m\varphi}(\rho) = \rho E_\rho(\rho, 0) = \frac{V_0}{\ln(b/a)} \left[1 + \sum_{j=1}^{J} E'_j f_j(\rho)\right] \tag{146}$$

$$R_m(\zeta_n \rho) = J_0(\zeta_n a) Y_m(\zeta_n \rho) - J_m(\zeta_n \rho) Y_0(\zeta_n a) \tag{147}$$

We need to pick a value for z_0/b and proceed to solve the linear system. This choice influences the solution and the resulting value of the total voltage across the gap from this choice. We solve the system

$$\sum_{j=1}^{J} E'_j \sum_{n=1}^{\infty} \left[\frac{\left\{J_0\left(j_{0,n}\rho_{j'+1/2}/b\right) - J_0\left(j_{0,n}\rho_{j'-1/2}/b\right)\right\}\left\{J_0\left(j_{0,n}\rho_{j+1/2}/b\right) - J_0\left(j_{0,n}\rho_{j-1/2}/b\right)\right\}}{j_{0,n}^3 J_1^2(j_{0,n})} \right.$$

$$\left. + \frac{\left\{R_0\left(\zeta_n\rho_{j'+1/2}\right) - R_0\left(\zeta_n\rho_{j'-1/2}\right)\right\}\left\{R_0\left(\zeta_n\rho_{j+1/2}\right) - R_0\left(\zeta_n\rho_{j-1/2}\right)\right\}}{(\zeta_n b)\left\{(\zeta_n b)^2 R_1^2(\zeta_n b) - (2/\pi)^2\right\}} \right]$$

$$= \frac{1}{2}(-z_0/b)\ln\left(\rho_{j'+1/2}/\rho_{j'-1/2}\right) + \sum_{n=1}^{\infty} \frac{\left\{J_0\left(j_{0,n}\rho_{j'+1/2}/b\right) - J_0\left(j_{0,n}\rho_{j'-1/2}/b\right)\right\} J_0(j_{0,n}a/b)}{j_{0,n}^3 J_1^2(j_{0,n})}\ ,\ j' = 1, ...J \tag{148}$$

To find the resulting total voltage from the center conductor to the outer conductor

$$V = \int_a^b E_\rho(\rho, 0)\, d\rho = \int_a^b \frac{V_0}{\rho \ln(b/a)} \left[1 + \sum_{j=1}^{J} E'_j f_j(\rho)\right] d\rho = V_0 \left[1 + \sum_{j=1}^{J} E'_j \ln\left(\rho_{j+1/2}/\rho_{j-1/2}\right) / \ln(b/a)\right] \tag{149}$$

Let us normalize the resulting electric fields, including the TEM mode unity term, by the bracketed quantity V/V_0

$$V_0 = V / \left[1 + \sum_{j=1}^{J} E'_j \ln\left(\rho_{j+1/2}/\rho_{j-1/2}\right) / \ln(b/a)\right] \tag{150}$$

The total field is then

$$E_\rho(\rho, 0) = \frac{V_0}{\rho \ln(b/a)} \left[1 + \sum_{j=1}^{J} E'_j f_j(\rho)\right]$$

$$= \frac{V}{\rho \ln(b/a)} \left[1 + \sum_{j=1}^{J} E'_j f_j(\rho)\right] / \left[1 + \sum_{j=1}^{J} E'_j \ln\left(\rho_{j+1/2}/\rho_{j-1/2}\right) / \ln(b/a)\right] \tag{151}$$

The modal coefficients are then given by

$$-\frac{V}{\ln(b/a)}\sum_{j=1}^{J}E'_j\left[\frac{R_0\left(\zeta_n\rho_{j+1/2}\right)-R_0\left(\zeta_n\rho_{j-1/2}\right)}{\left(\zeta_n b\right)^2R_1^2\left(\zeta_n b\right)-\left(2/\pi\right)^2}\right]\Big/\left[1+\sum_{j=1}^{J}E'_j\ln\left(\rho_{j+1/2}/\rho_{j-1/2}\right)/\ln(b/a)\right]=\frac{1}{2\varepsilon_0}A_n^- \tag{152}$$

$$-\frac{V}{\ln(b/a)}\frac{J_0\left(\xi_n a\right)}{j_{0,n}^2J_1^2\left(j_{0,n}\right)}+\frac{V}{\ln(b/a)}\sum_{j=1}^{J}E'_j\left[\frac{J_0\left(\xi_n\rho_{j+1/2}\right)-J_0\left(\xi_n\rho_{j-1/2}\right)}{j_{0,n}^2J_1^2\left(j_{0,n}\right)}\right]\Big/\left[1+\sum_{j=1}^{J}E'_j\ln\left(\rho_{j+1/2}/\rho_{j-1/2}\right)/\ln(b/a)\right]$$

$$=\frac{1}{2\varepsilon_0}A_n^+ \tag{153}$$

3.3 Electric Field At Terminated End Of Inner Conductor

The axial field is

$$D_z=\varepsilon_0E_z=-\frac{1}{\rho}\frac{\partial}{\partial\rho}\left(\rho A_{e\varphi}\right) \tag{154}$$

and using

$$\frac{1}{\rho}\frac{\partial}{\partial\rho}\left[\rho R_1\left(\zeta_n\rho\right)\right]=\zeta_n\left(\frac{\partial}{\zeta_n\partial\rho}+\frac{1}{\zeta_n\rho}\right)R_1\left(\zeta_n\rho\right)=\zeta_nR_0\left(\zeta_n\rho\right) \tag{155}$$

$$\varepsilon_0E_z=-\sum_{n=1}^{\infty}A_n^-\zeta_ne^{\zeta_nz}R_0\left(\zeta_n\rho\right)\ ,\ z<0\ ,\ a<\rho<b \tag{156}$$

$$\varepsilon_0E_z=-\sum_{n=1}^{\infty}A_n^+\xi_ne^{-\xi_nz}J_0\left(\xi_n\rho\right)\ ,\ z>0\ ,\ 0<\rho<b \tag{157}$$

The field at $z=+0$ and $\rho=0$ is then

$$E_z\left(0,+0\right)=-\sum_{n=1}^{\infty}\frac{1}{\varepsilon_0}A_n^+\xi_n$$

$$=\frac{2V_0}{b\ln(b/a)}\sum_{n=1}^{\infty}\frac{1}{j_{0,n}J_1^2\left(j_{0,n}\right)}\left[J_0\left(j_{0,n}a/b\right)-\sum_{j=1}^{J}E'_j\left\{J_0\left(j_{0,n}\rho_{j+1/2}/b\right)-J_0\left(j_{0,n}\rho_{j-1/2}/b\right)\right\}\right]$$

$$=\frac{2V}{b\ln(b/a)}\sum_{n=1}^{\infty}\frac{1}{j_{0,n}J_1^2\left(j_{0,n}\right)}\left[J_0\left(j_{0,n}a/b\right)-\sum_{j=1}^{J}E'_j\left\{J_0\left(j_{0,n}\rho_{j+1/2}/b\right)-J_0\left(j_{0,n}\rho_{j-1/2}/b\right)\right\}\right]$$

$$\Big/\left[1+\sum_{j=1}^{J}E'_j\ln\left(\rho_{j+1/2}/\rho_{j-1/2}\right)/\ln(b/a)\right] \tag{158}$$

The result for the summation in this equation, with $J = 100$ basis functions, is shown as the black curve in Figure 1. A fit is

$$E_z\left(0,+0\right) \approx \frac{2V}{b\ln\left(b/a\right)}\left[\left(b/a-1\right)/2+\left(b/a\right)^{3/2}/25\right] \tag{159}$$

where the bracketed part of this fit is shown as the gray curve in Figure 1. The approximate results from the radial field approximation, in the section below, are shown as the blue curve (the summation) and the green curve (the linear parenthetical expression) in Figure 1.

$$E_z^0\left(0,+0\right) = \frac{2V}{b\ln\left(b/a\right)}\sum_{n=1}^{\infty}\frac{J_0\left(j_{0,n}a/b\right)}{j_{0,n}J_1^2\left(j_{0,n}\right)} \approx \frac{2V}{b\ln\left(b/a\right)}\left(\frac{b}{2a}-0.4373\right) \tag{160}$$

Also shown as the red curve is the TEM mode (182)

$$E_\rho \approx \frac{V}{a\ln\left(b/a\right)} \tag{161}$$

This field at the terminal end of center conductor can be used to drive a connector at this point.

3.4 End Capacitance

It is sometimes of interest to determine the capacitance of the terminated center conductor (this exists in addition to the coaxial capacitance). The charge, assuming $A_{e\varphi}$ remains continuous from region to region is

$$Q = \int_S \underline{D}\cdot\underline{n}dS = -\oint_C \underline{A}_e\cdot\underline{d\ell} = -2\pi a A_{e\varphi}\left(a,-d_0\right) \tag{162}$$

where

$$A_{e\varphi}\left(a,-d_0\right) = -\frac{\varepsilon_0 V_0}{a\ln\left(b/a\right)}\left(-d_0-z_0\right)-\sum_{n=1}^{\infty}A_n^- e^{-\zeta_n d_0}R_1\left(\zeta_n a\right) \tag{163}$$

Taking d_0 to be large, and removing the dominant TEM field charge, the difference charge is then

$$\Delta Q = Q - \frac{2\pi\varepsilon_0 V_0 d_0}{\ln\left(b/a\right)} = \frac{2\pi\varepsilon_0 V_0\left(-z_0\right)}{\ln\left(b/a\right)} \tag{164}$$

We can write this charge correction in terms of the moment solution

$$\Delta Q = \frac{2\pi\varepsilon_0 V_0\left(-z_0\right)}{\ln\left(b/a\right)} = \frac{2\pi\varepsilon_0 V\left(-z_0\right)}{\ln\left(b/a\right)}\Big/\left[1+\sum_{j=1}^{J}E_j'\ln\left(\rho_{j+1/2}/\rho_{j-1/2}\right)/\ln\left(b/a\right)\right] \tag{165}$$

or difference capacitance

$$\begin{aligned}\Delta C = \Delta Q/V &= \frac{2\pi\varepsilon_0\left(-z_0\right)}{\ln\left(b/a\right)}\Big/\left[1+\sum_{j=1}^{J}E_j'\ln\left(\rho_{j+1/2}/\rho_{j-1/2}\right)/\ln\left(b/a\right)\right]\\ &= \frac{2\pi a\varepsilon_0}{\ln\left(b/a\right)}\left(-z_0/b\right)\left(b/a\right)/\left[1+\sum_{j=1}^{J}E_j'\ln\left(\rho_{j+1/2}/\rho_{j-1/2}\right)/\ln\left(b/a\right)\right]\end{aligned} \tag{166}$$

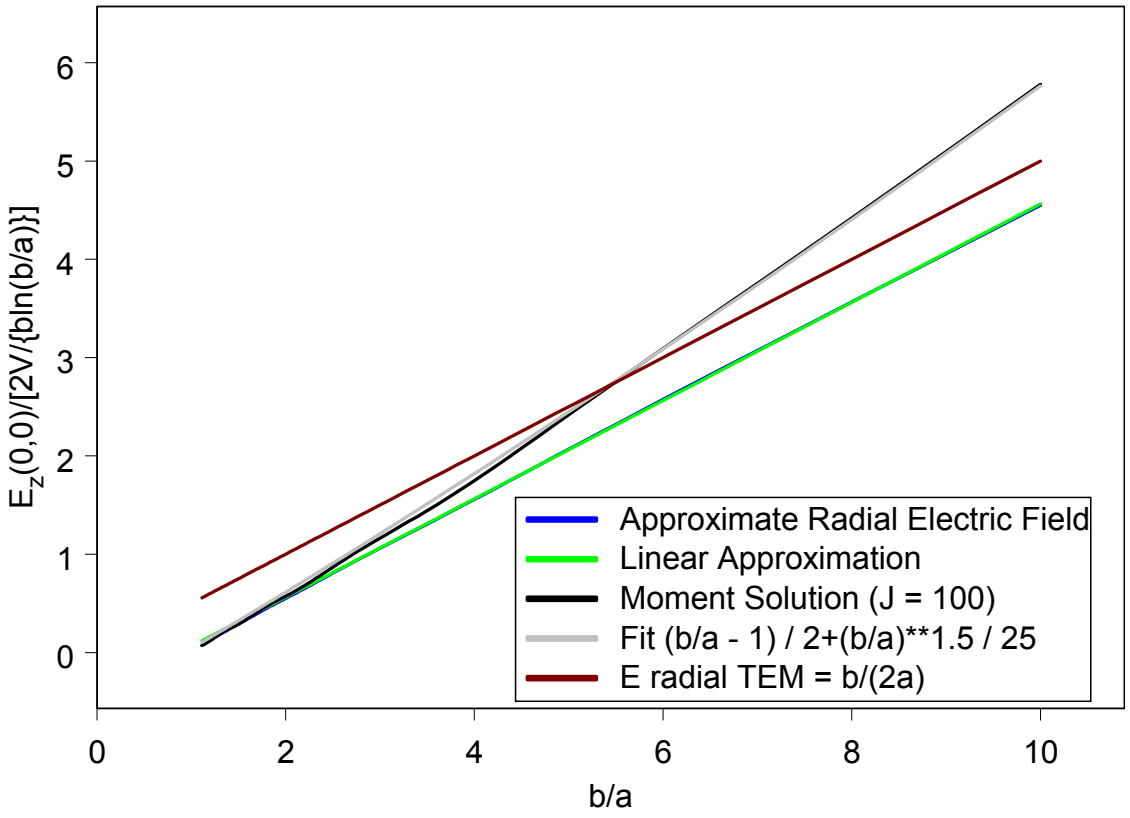

Figure 1: Comparison of sum involved in tip electric field at the center of the end of the solid coaxial center conductor as a function of ratio of outer-to-inner coaxial radii. The exact solution is the black curve; a simple fit is the gray curve. The blue curve uses an approximate radial electric field between the coax and cylindrical regions, which is proportional to the inverse radius; the green curve is a simple approximation to the tip field in the form of a linear function. The brown curve is a simple estimate based on the constant transverse electromagnetic mode.

which can be written as

$$\Delta C = \varepsilon_0 2\pi\rho_e \frac{(-z_0/b)}{(1-a/b)} \Big/ \left[1 + \sum_{j=1}^{J} E'_j \ln\left(\rho_{j+1/2}/\rho_{j-1/2}\right) / \ln(b/a)\right] \tag{167}$$

with [5]

$$\rho_e = (b-a) / \ln(b/a) \tag{168}$$

A fit is

$$\Delta C \approx 2\varepsilon_0\rho_e \left[\frac{1}{2.3}\ln\left(\frac{\pi}{\ln(b/a)}\right) + 0.0125b/a\right] = 2\varepsilon_0\rho_e \left[\frac{1}{2.3}\left\{\ln\left(\frac{\pi e\rho_e/4}{b-a}\right) + 2\ln 2 - 1\right\} + 0.0125b/a\right] \tag{169}$$

The capacitance using the approximate radial field, from the section below, is

$$\Delta C^0 = \frac{2\pi a\varepsilon_0}{\ln(b/a)} 2\sum_{n=1}^{\infty}\left[\frac{J_0(j_{0,n}a/b)}{j_{0,n}J_1(j_{0,n})}\right]^2 = \varepsilon_0 2\pi\rho_e \frac{2a/b}{(1-a/b)}\sum_{n=1}^{\infty}\left[\frac{J_0(j_{0,n}a/b)}{j_{0,n}J_1(j_{0,n})}\right]^2 \tag{170}$$

Figure 2 shows the moment solution using $J = 100$ as the black curve. The fit is shown as the green curve. This result using the approximate radial electric field in the next subsections is the gray curve.

3.5 Approximation For Radial Electric Field Or Magnetic Current At Terminated Inner Conductor

Suppose we approximate the radial field (or magnetic current) in the coaxial dominant mode as

$$E_\rho \approx \frac{V}{\rho\ln(b/a)}\ ,\ a<\rho<b\ ,\ z>0 \tag{171}$$

and use

$$D_\rho = \varepsilon_0 E_\rho = \frac{\partial}{\partial z}A_{e\varphi} = -\sum_{n=1}^{\infty} A_n^+ \xi_n e^{-\xi_n z} J_1(\xi_n\rho)\ ,\ z>0 \tag{172}$$

to set

$$\frac{\varepsilon_0 V}{\rho\ln(b/a)} \approx -\sum_{n=1}^{\infty} A_n^+ \xi_n J_1(\xi_n\rho)\ ,\ a<\rho<b \tag{173}$$

we can use orthogonality of the Bessel functions to write

$$\int_0^b J_1(\xi_n\rho)\, J_1(\xi_{n'}\rho)\,\rho d\rho = b^2\int_0^1 J_1(j_{0,n}u)\, J_1(j_{0,n'}u)\, u du = \frac{b^2}{2}\left[J_1(j_{0,n})\right]^2\delta_{nn'} \tag{174}$$

$$\frac{1}{\rho}\frac{\partial}{\partial\rho}\left[\rho J_1(\xi_n\rho)\right] = \xi_n\left(\frac{\partial}{\xi_n\partial\rho} + \frac{1}{\xi_n\rho}\right)J_1(\xi_n\rho) = \frac{1}{\rho}\left[J_1(\xi_n\rho) + \xi_n\rho J_1'(\xi_n\rho)\right] = \xi_n J_0(\xi_n\rho) \tag{175}$$

$$J_1(j_{0,n}) + j_{0,n}J_1'(j_{0,n}) = j_{0,n}J_0(j_{0,n}) = 0 \tag{176}$$

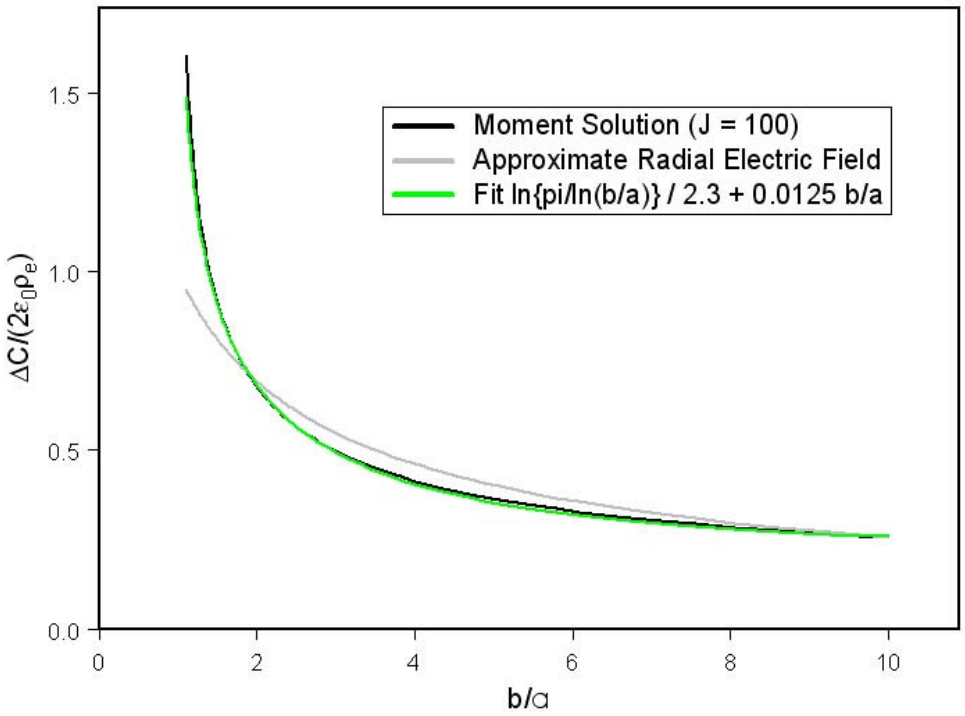

Figure 2: Correction capacitance (addition to simple coaxial capacitance) due to termination of coaxial center conductor. Black curve is exact solution; green curve is simple fit. Gray curve is approximate result using a radial electric field at the junction between coax and cylinder which is proportional to the inverse of the radius.

Then

$$\frac{\varepsilon_0 V}{\ln(b/a)}\int_a^b J_1(\xi_n\rho)\,d\rho = \frac{\varepsilon_0 V}{\ln(b/a)}\frac{1}{\xi_n}\left[J_0(\xi_n a) - J_0(\xi_n b)\right] \approx -A_n^+\xi_n\frac{b^2}{2}\left[J_1(j_{0,n})\right]^2 \tag{177}$$

or

$$A_n^+\frac{1}{2}j_{0,n}^2\left[J_1(j_{0,n})\right]^2 \approx \left[J_0(j_{0,n}) - J_0(j_{0,n}a/b)\right]\frac{\varepsilon_0 V}{\ln(b/a)} = -J_0(j_{0,n}a/b)\frac{\varepsilon_0 V}{\ln(b/a)} \tag{178}$$

and thus

$$E_z(0,+0) \approx E_z^0(0,+0) = \frac{2V}{b\ln(b/a)}\sum_{n=1}^{\infty}\frac{J_0(j_{0,n}a/b)}{\left[J_1(j_{0,n})\right]^2 j_{0,n}} \tag{179}$$

we also find

$$\sum_{n=1}^{\infty}\frac{J_0(j_{0,n}a/b)}{\left[J_1(j_{0,n})\right]^2 j_{0,n}} \approx \frac{b}{2a} - 0.4373 \approx \frac{b}{2a} - 0.8747/2 \tag{180}$$

Using this linear approximation we therefore obtain

$$E_z^0(0,+0) \approx \frac{V}{\ln(b/a)}\left(1/a - 0.8747/b\right) \tag{181}$$

Noting that the radial electric field on the center conductor for the TEM mode is

$$E_\rho \approx \frac{V}{a\ln(b/a)} \tag{182}$$

we see that this is a bound on the tip electric field (181), with correction factor $1 - 0.8747a/b$. This simple coaxial result (182) is only slightly below the numerical solution fit (159) for $b/a > 6$.

Remainder Of Summation A remainder has been added to improve convergence of the modal summation

$$j_{0,n} \sim (n - 1/4)\,\pi \tag{183}$$

$$J_0(j_{0,n}a/b) \sim \sqrt{\frac{2}{\pi j_{0,n}a/b}}\cos(j_{0,n}a/b - \pi/4) \tag{184}$$

$$J_1(j_{0,n}) \sim \sqrt{\frac{2}{\pi j_{0,n}}}\cos(j_{0,n} - 3\pi/4) \sim \sqrt{\frac{2}{\pi j_{0,n}}}(-1)^{n-1} \tag{185}$$

$$\frac{2V}{b\ln(b/a)}\sqrt{\frac{\pi b}{2a}}\sum_{n=N+1}^{\infty}\frac{1}{\sqrt{j_{0,1}}}\cos(j_{0,n}a/b - \pi/4) \sim \frac{2V}{b\ln(b/a)}\sqrt{\frac{b}{2a}}\sum_{n=N+1}^{\infty}\frac{1}{\sqrt{n-1/4}}\cos((n-1/4)\,\pi a/b - \pi/4)$$

$$\sim \frac{2V}{b\ln(b/a)}\sqrt{\frac{b}{2a}}\left[\cos((a/b+1)\,\pi/4)\sum_{n=N+1}^{\infty}\frac{1}{\sqrt{n}}\cos(n\pi a/b) - \sin((a/b+1)\,\pi/4)\sum_{n=N+1}^{\infty}\frac{1}{\sqrt{n}}\sin(n\pi a/b)\right] \tag{186}$$

$$\cos\left(\left(n-1/4\right)\pi a/b-\pi/4\right)=\cos\left(n\pi a/b\right)\cos\left(\left(a/b+1\right)\pi/4\right)-\sin\left(n\pi a/b\right)\sin\left(\left(a/b+1\right)\pi/4\right) \tag{187}$$

$$\sum_{n=1}^{\infty}\frac{J_0\left(j_{0,n}a/b\right)}{\left[J_1\left(j_{0,n}\right)\right]^2 j_{0,1}}\sim\sum_{n=1}^{N}\frac{J_0\left(j_{0,n}a/b\right)}{\left[J_1\left(j_{0,n}\right)\right]^2 j_{0,1}}+\sqrt{\frac{b}{2a}}\sum_{n=N+1}^{\infty}\frac{1}{\sqrt{n-1/4}}\cos\left(\left(n-1/4\right)\pi a/b-\pi/4\right) \tag{188}$$

3.5.1 Capacitance Using Approximate Radial Electric Field

The additional capacitance at the terminating coax, using the radial electric field approximation, is

$$E_\rho\approx\frac{V}{\rho\ln\left(b/a\right)}\ ,\ a<\rho<b\ ,\ z>0 \tag{189}$$

$$Q=\int_S\underline{D}\cdot\underline{n}dS=-\oint_C\underline{A}_e\cdot\underline{d\ell}=-2\pi aA_{e\varphi}\left(a,+0\right)=\Delta Q^0 \tag{190}$$

$$A_{e\varphi}=\sum_{n=1}^{\infty}A_n^+e^{-\xi_n z}J_1\left(\xi_n\rho\right)\ ,\ z>0 \tag{191}$$

$$A_n^+\approx-\frac{J_0\left(j_{0,n}a/b\right)}{j_{0,n}^2\left[J_1\left(j_{0,n}\right)\right]^2}\frac{2\varepsilon_0V}{\ln\left(b/a\right)} \tag{192}$$

$$\Delta Q^0=-2\pi a\sum_{n=1}^{\infty}A_n^+J_1\left(j_{0,n}a/b\right)=2\pi a\frac{2\varepsilon_0V}{\ln\left(b/a\right)}\sum_{n=1}^{\infty}\left[\frac{J_0\left(j_{0,n}a/b\right)}{j_{0,n}J_1\left(j_{0,n}\right)}\right]^2 \tag{193}$$

$$\Delta C^0=2a\varepsilon_0\frac{2\pi}{\ln\left(b/a\right)}\sum_{n=1}^{\infty}\left[\frac{J_0\left(j_{0,n}a/b\right)}{j_{0,n}J_1\left(j_{0,n}\right)}\right]^2=2\varepsilon_0\rho_e\frac{2\pi a/b}{\left(1-a/b\right)}\sum_{n=1}^{\infty}\left[\frac{J_0\left(j_{0,n}a/b\right)}{j_{0,n}J_1\left(j_{0,n}\right)}\right]^2 \tag{194}$$

$$J_0\left(j_{0,n}a/b\right)\sim J_0\left(j_{0,n}\right)+\left(1-a/b\right)J_1\left(j_{0,1}\right)+\cdots \tag{195}$$

$$\rho_e=\left(b-a\right)/\ln\left(b/a\right) \tag{196}$$

The limit of a small coaxial gap is

$$\Delta C^0\sim2\varepsilon_0\rho_e2\pi\left(a/b\right)\left(1-a/b\right)\sum_{n=1}^{\infty}\frac{1}{j_{0,n}^2}=2\varepsilon_0\rho_e\frac{\pi}{2}\left(a/b\right)\left(1-a/b\right)\ ,\ a/b\to1 \tag{197}$$

where

$$\sum_{n=1}^{\infty}\frac{1}{j_{0,n}^2}=1/4 \tag{198}$$

3.6 Connector Cover Charge And Current

If a connector is capped at the terminal end of the center conductor, this cap substantially reduces the voltage and resulting electric field incident on the underlying pins. One way to estimate its effect is to first estimate the charge deposited by the electric field at the center conductor tip

$$Q_{sc}^{cap} = A_e^{cap} \varepsilon_0 E_z \left(0, +0\right) \tag{199}$$

The electric current from this cap to the center conductor end (crossing to the connector base) is then the time derivative of this charge

$$I_{sc}^{cap} = \frac{\partial}{\partial t} Q_{sc}^{cap} \leq \frac{1}{\tau_r} Q_{sc}^{cap} = \frac{1}{\tau_r} A_e^{cap} \varepsilon_0 E_z \left(0, +0\right) \tag{200}$$

An estimate for the area A_e^{cap} can be taken as the connector surface area. In this electric field case we can take

$$K_{sc}^{cap} \approx I_{sc}^{cap} / \left(2\pi a_{cap}\right) \tag{201}$$

Because of the permittivity ε_0 factor in the charge this is a relatively small current and current density. The magnetic field driven current density (367) is assumed to be larger.

3.7 Cap To Connector Inductance/Resistance

Because the connector cap has an inductance to the base of the connector, there is a voltage developed between the connector cap and the connector base. We can estimate the maximum values around the perimeter as [1]

$$V_{\max} = V_{\max}^{ext} + V_{\max}^{int} + V_{pin}^{int} \tag{202}$$

$$V_{\max}^{ext} = L_{\max}^{cap} 2h_{cap} \frac{d}{dt} K_{sc}^{cap} \leq L_{\max}^{cap} 2h_{cap} K_{sc}^{cap} / \tau_r \tag{203}$$

$$\begin{aligned} \frac{1}{2} V_{\max}^{int} &= \frac{L_{\max}^{cap}}{\mu_0 w_{cap}} \sqrt{\mu_{cap}/\sigma_{cap}} \frac{d^{1/2}}{dt^{1/2}} I_{pin} \leq \sqrt{\frac{4\mu_{cap} t}{\pi \sigma_{cap}}} \frac{L_{\max}^{cap}}{\mu_0 w_{cap}} I_{pin} / \tau_r \\ &= \frac{L_{\max}^{cap}}{\mu_0 w_{cap}} \sqrt{\mu_{cap}/\sigma_{cap}} 2h_{cap} \frac{d^{1/2}}{dt^{1/2}} K_{sc}^{cap} \leq \sqrt{\frac{4\mu_{cap} t}{\pi \sigma_{cap}}} \frac{L_{\max}^{cap}}{\mu_0 w_{cap}} 2h_{cap} K_{sc}^{cap} / \tau_r \end{aligned} \tag{204}$$

with maximum in time

$$\frac{1}{2} V_{\max}^{int} \leq \sqrt{\frac{4\mu_{cap}\tau_r}{\pi \sigma_{cap}}} \frac{L_{\max}^{cap}}{\mu_0 w_{cap}} 2h_{cap} K_{sc}^{cap} / \tau_r \tag{205}$$

where μ_{cap} and σ_{cap} are the magnetic permeability and electrical conductivity of the connector cap material (and the connector base is assumed to be the same material here, although the formulas could easily be generalized). The penetration depth is (here using general symbols μ and σ)

$$\delta = \sqrt{2/\left(\omega\mu\sigma\right)} \rightarrow \sqrt{2\tau_r/\left(\mu\sigma\right)} \tag{206}$$

There is also an internal voltage contribution due to the pin (between cap and connector base) itself. If the current is confined to the surface of the pin for the rise time region

$$V_{pin}^{int} = \frac{w_{cap}}{2\pi a_{pin}} \sqrt{\mu_{pin}/\sigma_{pin}} \frac{\partial^{1/2}}{\partial t^{1/2}} I_{pin}(t) = \frac{w_{cap}}{2\pi a_{pin}} \sqrt{\frac{4\mu_{pin} t}{\pi \sigma_{pin}}} (I_{pin}/\tau_r) \tag{207}$$

with maximum value

$$V_{pin}^{int} \leq \frac{w_{cap}}{2\pi a_{pin}} \sqrt{\frac{4\mu_{pin}\tau_r}{\pi \sigma_{pin}}} (I_{pin}/\tau_r) \tag{208}$$

where μ_{pin} and σ_{pin} are the magnetic permeability and conductivity of the pin material. If the current is uniformly distributed in the pin this changes to the resistive value

$$V_{pin}^{int} \leq \frac{w_{cap} I_{pin}}{\pi a_{pin}^2 \sigma_{pin}} \tag{209}$$

The two contributions compare as

$$\text{(skin effect) } \sqrt{\frac{\mu_{pin}\sigma_{pin}}{\pi \tau_r}} \Longleftrightarrow \frac{1}{a_{pin}} \text{ (resistive)} \tag{210}$$

Therefore using the skin effect form

$$V_{\max} \leq \left[L_{\max}^{cap} \left(1 + \sqrt{\frac{4\mu_{cap}\tau_r}{\pi\sigma_{cap}}} \frac{2}{\mu_0 w_{cap}} \right) + \frac{w_{cap}}{2\pi a_{pin}} \sqrt{\frac{4\mu_{pin}\tau_r}{\pi\sigma_{pin}}} \right] 2h_{cap} K_{sc}^{cap}/\tau_r \tag{211}$$

An estimate for this cap inductance can be made due to the cap-to-connector base slots [1], [6]

$$L_{\max}^{cap} \sim \frac{\mu_0 w_{cap}}{2\pi} \ln\left(\frac{h_{cap}}{\pi a_{pin}} \right) \ , \ d_{cap} >> \ell_{cap} = 2h_{cap} \tag{212}$$

$$L_{\max}^{cap} \sim \frac{1}{4}\mu_0 h_{cap} \frac{w_{cap}}{d_{cap}} + \frac{\mu_0 w_{cap}}{2\pi} \ln\left[\frac{d_{cap}/(2\pi a_{pin})}{\sqrt{\cos(\pi f_{pin}/d_{cap}) + \left(\frac{\pi a_{pin}}{2d_{cap}}\right)^2}} \right] \ , \ d_{cap} < h_{cap} \tag{213}$$

where $2h_{cap} = \ell_{cap}$ is the distance between pin contacts, d_{cap} is the overlap depth, w_{cap} is the gap width, a_{pin} is the pin radius, and f_{pin} is the displacement of the pins from the depth center toward the interior of the connector. For $f_{pin} = 0$ a function which incorporates both these limits, and remains uniformly valid, is [1]

$$L_{\max}^{cap} \approx \frac{1}{4}\mu_0 h_{cap} \frac{w_{cap}}{d_{cap}} + \frac{\mu_0 w_{cap}}{2\pi} \left[\ln\left(\frac{d_{cap}/2}{h_{cap} + d_{cap}/2} \right) - \ln\left(1 - e^{-\pi a_{pin}/h_{cap}} \right) \right] \ , \ f_{pin} = 0 \tag{214}$$

The variation of the voltage around the cap perimeter is a somewhat weak function of the azimuth angle when the depth is larger than the half length, the pin radius is small, and the bolt is not near the transmitted slot outlet.

Near the outer radius of the cap, but interior to the connector, the voltage appears at the top of the cap, where the cap insulator exists. This voltage spreads out to develop the electric field near the pins. We estimate the electric field at the pins by using the a parallel plate formula

$$h_{conn} E_{cap} \sim V_{\max}^{cap} \tag{215}$$

where h_{conn} is the height of the cap above the base of the pins. If the insulator is foam with a dielectric constant near unity, the height h_{conn} is the distance to the cap metallic surface. Alternatively, if it is a solid dielectric this height should be reduced somewhat (the thickness of the insulator reduced by the inverse of the dielectric constant) to account for the dielectric constant of the insulator.

3.8 Connector Pin Voltage

Treating the connector pin as a monopole with effective height h_e, the electric field (181) gives a connector pin open circuit voltage

$$V_{oc}^{pin} = h_e E_z\left(0, +0\right) \rightarrow h_e E_{cap} \tag{216}$$

where the final expression uses the preceding interior cap electric field.

3.8.1 Pin-Wire Voltages

The Thevinen drive circuit with the preceding connector pin open circuit voltage has an accompanying large (nearly open circuited) capacitive impedance element. At the low frequencies associated with lightning, this impedance element is nearly open, and hence for typical attached load impedances the actual voltage delivered to a load V_L will often be reduced. We often do not really know the load impedance of a particular pin, however, the interior intervening cable capacitive reactance alone should reduce the voltage delivered to the load. Consider a capacitive voltage divider consisting of the pin capacitance (to connector) of the Thevinen source and the cable capacitance of an interior line to the shield. The capacitance of a short monopole of height h_p with radius a_p above a ground plane is

$$C_p \lesssim \frac{4\pi\varepsilon_0 h_p}{\Omega_{ep}} = h_p 2\pi\varepsilon_0 / \ln\left[\left(h_p/e\right)/a_p\right] \tag{217}$$

where

$$\Omega_{ep} = 2\ln\left(2h_p/a_p\right) - 2\left(\ln 2 + 1\right) \tag{218}$$

The capacitance of an interior cable run can be underestimated (due to neglect of the other lines) by the eccentric coax formula

$$C_w \lesssim \ell_w 2\pi\varepsilon_0 / \text{Arccosh}\left(\frac{a_{coax}^2 + b_{coax}^2 - d_{coax}^2}{2a_{coax}b_{coax}}\right) \tag{219}$$

where ℓ_w is the wire length in the coax, a_{coax} is the radius of the wire (connected to the pin of interest) in the coax, b_{coax} is the radius of the shield return (this could also include the effect of the other wires in the cable in which case it is smaller than the shield radius, d_{coax} is the offset between the pin wire center and the shield center. For a center coax $d_{coax} = 0$ and

$$C_w \rightarrow \ell_w 2\pi\varepsilon_0 / \ln\left(\frac{b_{coax}}{a_{coax}}\right) \tag{220}$$

Because we expect that the multiplier of the coaxial capacitance per unit length ℓ_w is very large compared to the monopole pin multiplier h_p, we also expect that C_w is very large compared to C_p. Hence we expect that the pin voltage, even with an open circuit at the other end of the coax, to be

$$V_L \lesssim V_{oc}^{pin} \frac{C_p}{C_p + C_w} \tag{221}$$

We expect the ratio to be in the range $C_w/C_p > 10$ and hence the voltage delivered to a high impedance load to still be considerably reduced.

3.9 Door To Coaxial Capacitance Element

The induced charge or capacitance matrix element to the center coaxial conductor, resulting from the door to outer container voltage, is now found. The charge on the cylindrical center conductor, due to the door voltage, is found by driving the shorted coax (held at the potential of the outer cylinder) with two magnetic current loops to support the door voltage V_d (one at radius a and one at radius b). Using

$$\underline{K}_m = -\underline{n} \times (\underline{E}_2 - \underline{E}_1) \tag{222}$$

we can image the magnetic currents and remove the door, extending the coaxial region beyond the door location $z = -h$. Then we have magnetic current loops

$$\begin{aligned} K_{m\varphi} &= 2V_d \delta(z+h) \ , \ \rho = b \\ &= -2V_d \delta(z+h) \ , \ \rho = a \end{aligned} \tag{223}$$

The representation is taken as (there is no $1/\rho$ term since the center conductor is assumed to be shorted to chassis, or the outer cylinder, here)

$$\begin{aligned} A_{e\varphi} &= \sum_{n=1}^{\infty} A_n^{+h} e^{-\zeta_n (z+h)} R_1(\zeta_n \rho) \ , \ z > -h \\ &= \sum_{n=1}^{\infty} A_n^{-h} e^{\zeta_n (z+h)} R_1(\zeta_n \rho) \ , \ z < -h \end{aligned} \tag{224}$$

where

$$R_1(\zeta_n \rho) = J_0(\zeta_n a) Y_1(\zeta_n \rho) - J_1(\zeta_n \rho) Y_0(\zeta_n a) \tag{225}$$

$$\left[\frac{1}{\rho}\frac{\partial}{\partial \rho}(\rho A_{e\varphi})\right]_{\rho=b} = -\varepsilon_0 E_z(\rho = b) = 0 = -\varepsilon_0 E_z(\rho = a) = \left[\frac{1}{\rho}\frac{\partial}{\partial \rho}(\rho A_{e\varphi})\right]_{\rho=a} \ , \ z > -h \tag{226}$$

$$\frac{1}{\rho}\frac{\partial}{\partial \rho}[\rho R_1(\zeta_n \rho)] = \zeta_n \left(\frac{\partial}{\zeta_n \partial \rho} + \frac{1}{\zeta_n \rho}\right) R_1(\zeta_n \rho) = \zeta_n R_0(\zeta_n \rho) \tag{227}$$

$$R_0(\zeta_n \rho) = J_0(\zeta_n a) Y_0(\zeta_n \rho) - J_0(\zeta_n \rho) Y_0(\zeta_n a) \tag{228}$$

$$R_0(\zeta_n a) = 0 \tag{229}$$

$$R_0(\zeta_n b) = J_0(\zeta_n a) Y_0(\zeta_n b) - J_0(\zeta_n b) Y_0(\zeta_n a) = 0 \tag{230}$$

Then the fields are

$$D_z(\rho, z) = \varepsilon_0 E_z(\rho, z) = -\frac{1}{\rho}\frac{\partial}{\partial \rho}(\rho A_{e\varphi}) = -\sum_{n=1}^{\infty} A_n^{+h} e^{-\zeta_n (z+h)} \zeta_n R_0(\zeta_n \rho) \ , \ z > -h \tag{231}$$

$$D_\rho = \varepsilon_0 E_\rho = \frac{\partial}{\partial z} A_{e\varphi} = -\sum_{n=1}^{\infty} A_n^{+h} e^{-\zeta_n (z+h)} \zeta_n R_1 (\zeta_n \rho) \ , \ z > -h \tag{232}$$

We now match

$$\varepsilon_0 E_\rho (\rho, -h) = \varepsilon_0 V_d \delta (\rho - b) - \varepsilon_0 V_d \delta (\rho - a) = -\sum_{n=1}^{\infty} A_n^{+h} \zeta_n R_1 (\zeta_n \rho) \tag{233}$$

and use orthogonality

$$\int_a^b R_1 (\zeta_n \rho) R_1 (\zeta_{n'} \rho) \rho d\rho = \delta_{nn'} \left[\frac{1}{2} \rho^2 \left\{ \left(1 - \frac{1}{\zeta_n^2 \rho^2} \right) R_1^2 (\zeta_n \rho) + R_1'^2 (\zeta_n \rho) \right\} \right]_a^b$$

$$= \delta_{nn'} \left[\frac{1}{2} b^2 \left\{ \left(1 - \frac{1}{\zeta_n^2 b^2} \right) R_1^2 (\zeta_n b) + R_1'^2 (\zeta_n b) \right\} - \frac{1}{2} a^2 \left\{ \left(1 - \frac{1}{\zeta_n^2 a^2} \right) R_1^2 (\zeta_n a) + R_1'^2 (\zeta_n a) \right\} \right] \tag{234}$$

where

$$R_m (\zeta_n \rho) = J_0 (\zeta_n a) Y_m (\zeta_n \rho) - J_m (\zeta_n \rho) Y_0 (\zeta_n a) \tag{235}$$

and the first required condition for orthogonality is

$$h_1 \zeta_n R_2 (\zeta_n b) - h_2 R_1 (\zeta_n b) = 0$$

$$= h_1 \zeta_n \left[J_0 (\zeta_n a) Y_2 (\zeta_n b) - J_2 (\zeta_n b) Y_0 (\zeta_n a) \right] - h_2 \left[J_0 (\zeta_n a) Y_1 (\zeta_n b) - J_1 (\zeta_n b) Y_0 (\zeta_n a) \right] \tag{236}$$

With $h_1 = b$ and $h_2 = 2$

$$\zeta_n b J_2 (\zeta_n b) - 2 J_1 (\zeta_n b) = -\zeta_n b J_0 (\zeta_n b) \tag{237}$$

$$\zeta_n b Y_2 (\zeta_n b) - 2 Y_1 (\zeta_n b) = -\zeta_n b Y_0 (\zeta_n b) \tag{238}$$

$$h_1 \zeta_n R_2 (\zeta_n b) - h_2 R_1 (\zeta_n b) = -\zeta_n b \left[J_0 (\zeta_n a) Y_0 (\zeta_n b) - J_0 (\zeta_n b) Y_0 (\zeta_n a) \right] = -\zeta_n b R_0 (\zeta_n b) = 0 \tag{239}$$

The second condition for orthogonality is

$$k_1 \zeta_n R_2 (\zeta_n a) - k_2 R_1 (\zeta_n a) = 0$$

$$= k_1 \zeta_n \left[J_0 (\zeta_n a) Y_2 (\zeta_n a) - J_2 (\zeta_n a) Y_0 (\zeta_n a) \right] - k_2 \left[J_0 (\zeta_n a) Y_1 (\zeta_n a) - J_1 (\zeta_n a) Y_0 (\zeta_n a) \right] \tag{240}$$

With $k_1 = a$ and $k_2 = 2$

$$\zeta_n a J_2 (\zeta_n a) - 2 J_1 (\zeta_n a) = -\zeta_n a J_0 (\zeta_n a) \tag{241}$$

$$\zeta_n a Y_2(\zeta_n a) - 2Y_1(\zeta_n a) = -\zeta_n a Y_0(\zeta_n a) \tag{242}$$

$$k_1\zeta_n R_2(\zeta_n a) - k_2 R_1(\zeta_n a) = -\zeta_n a\left[J_0(\zeta_n a) Y_0(\zeta_n a) - J_0(\zeta_n a) Y_0(\zeta_n a)\right] = -\zeta_n a R_0(\zeta_n a) = 0 \tag{243}$$

Noting that h_1 and h_2 are not both zero, k_1 and k_2 are not both zero, we see that the orthogonality conditions are met. Then we find

$$\varepsilon_0 V_d \int_a^b R_1(\zeta_n\rho)\left[\delta(\rho-b) - \delta(\rho-a)\right]\rho d\rho = \varepsilon_0 V_d\left[bR_1(\zeta_n b) - aR_1(\zeta_n a)\right] = -A_n^{+h}\zeta_n \int_a^b R_1^2(\zeta_n\rho)\,\rho d\rho$$

$$= -A_n^{+h}\zeta_n\left[\frac{1}{2}b^2\left\{\left(1-\frac{1}{\zeta_n^2 b^2}\right)R_1^2(\zeta_n b) + R_1'^2(\zeta_n b)\right\} - \frac{1}{2}a^2\left\{\left(1-\frac{1}{\zeta_n^2 a^2}\right)R_1^2(\zeta_n a) + R_1'^2(\zeta_n a)\right\}\right] \tag{244}$$

$$R_1'(\zeta_n\rho) = J_0(\zeta_n a) Y_1'(\zeta_n\rho) - J_1'(\zeta_n\rho) Y_0(\zeta_n a)$$

$$= J_0(\zeta_n a) Y_0(\zeta_n\rho) - J_0(\zeta_n\rho) Y_0(\zeta_n a) + \frac{1}{\zeta_n\rho}\left\{J_1(\zeta_n\rho) Y_0(\zeta_n a) - J_0(\zeta_n a) Y_1(\zeta_n\rho)\right\} \tag{245}$$

$$R_1'(\zeta_n a) = \frac{2}{\pi(\zeta_n a)^2} \tag{246}$$

$$R_1'(\zeta_n b) = R_0(\zeta_n b) - R_1(\zeta_n b)/(\zeta_n b) = -R_1(\zeta_n b)/(\zeta_n b) \tag{247}$$

$$R_1(\zeta_n b) = J_0(\zeta_n a) Y_1(\zeta_n b) - J_1(\zeta_n b) Y_0(\zeta_n a) \tag{248}$$

$$R_1(\zeta_n a) = J_0(\zeta_n a) Y_1(\zeta_n a) - J_1(\zeta_n a) Y_0(\zeta_n a) = -\frac{2}{\pi\zeta_n a} \tag{249}$$

and then

$$2\varepsilon_0 V_d/\left[(\zeta_n b) R_1(\zeta_n b) - 2/\pi\right] = -A_n^{+h} \tag{250}$$

Now with these coefficients A_n^{+h} we can determine the values of A_{ez}. The local induced charge on the center conductor is (here the surface S covers the cylindrical surface of the center conductor and the contour C bounds the surface S (directed to keep the surface on the left as we traverse the contour in a counter-clockwise sense)

$$Q_e = \int_S \underline{D}\cdot\underline{n}dS = -\oint_C \underline{A}_e\cdot\underline{d\ell} = 2\pi a\left[A_{e\varphi}(\rho=a, z\to+\infty) - A_{e\varphi}(\rho=a, z=+\Delta-h)\right]$$

$$= -2\pi a\sum_{n=1}^{\infty} A_n^{+h} e^{-\zeta_n\Delta} R_1(\zeta_n a) \tag{251}$$

or

$$-Q_e/V_d = 4\pi a\varepsilon_0 \sum_{n=1}^{\infty} e^{-\zeta_n \Delta} \frac{2/\left(\pi\zeta_n a\right)}{\left(\zeta_n b\right) R_1\left(\zeta_n b\right) - 2/\pi} \tag{252}$$

The gap can be inserted by taking [7] (the gap in the reference is twice the gap to the door ground plane here $2g$)

$$\Delta = 2\left(2g\right)/\left(\pi e\right) \tag{253}$$

and adding the parallel plate end cap capacitance

$$C_{struc} \approx \varepsilon_0 \pi a^2/g - Q_e/V_d \tag{254}$$

We also take the door drive voltage as the average

$$V_d = \langle V_{tot} \rangle \tag{255}$$

The spacing is taken equal to the gap equivalent radius $\Delta = 2\left(2g\right)/\left(\pi e\right)$. If we choose a gap value $g_0 << a$ with $\Delta_0 = 2\left(2g_0\right)/\left(\pi e\right)$, we can estimate the variation about this value by [7] (the voltage in the reference is twice the voltage to the ground plane here and hence the correction doubles)

$$-Q_e/V_d = -\left(Q_e/V_d\right)_0 + \varepsilon_0 2\pi a \frac{2}{\pi} \ln\left(g_0/g\right) \tag{256}$$

Then

$$-\left(Q_e/V_d\right)/\left(2\pi a\varepsilon_0\right) = 2\sum_{n=1}^{\infty} e^{-\zeta_n \Delta_0} \frac{2/\left(\pi\zeta_n a\right)}{\left(\zeta_n b\right) R_1\left(\zeta_n b\right) - 2/\pi} + \frac{2}{\pi} \ln\left(g_0/g\right) \tag{257}$$

Picking the value $2g_0/a = 0.01$ we find

$$2\sum_{n=1}^{\infty} e^{-\zeta_n \Delta_0} \frac{2/\left(\pi\zeta_n a\right)}{\left(\zeta_n b\right) R_1\left(\zeta_n b\right) - 2/\pi} \approx \ln\left(\left(b/a\right)^2 - 1\right) + 2 + 2\left(b/a\right)^{-3/2} \tag{258}$$

This coaxial function summation is shown as the black curve in Figure 3 and the simple fit on the right hand side is shown as the gray curve.

Using this simple fit we then have

$$C_{struc} \approx \varepsilon_0 2\pi a \left[\ln\left(\left(b/a\right)^2 - 1\right) + 2 + 2\left(b/a\right)^{-3/2} + \frac{2}{\pi} \ln\left(g_0/g\right) + a/\left(2g\right)\right] \tag{259}$$

We can choose the center conductor radius here to be different $a \to a_0$ than at the other end of the coax

$$C_{struc} \approx \varepsilon_0 2\pi a_0 \left[\ln\left(\left(b/a_0\right)^2 - 1\right) + 2 + 2\left(b/a_0\right)^{-3/2} + \frac{2}{\pi} \ln\left(\frac{a_0/100}{2g}\right) + a_0/\left(2g\right)\right] \tag{260}$$

We can take g up to $O\left(a_0\right)$, with $b/a \geq 2$, with reasonable accuracy $O\left(10\%\right)$.

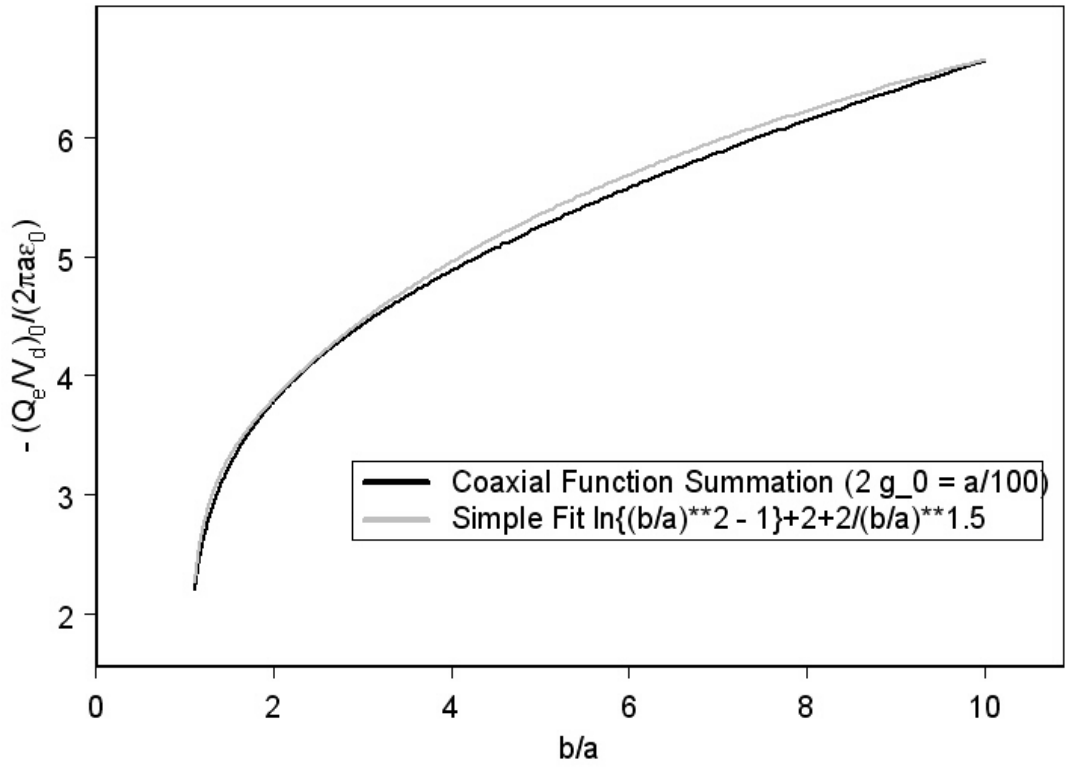

Figure 3: The electric charge on the coaxial center conductor (held at the potential of the outer cylinder) when the end door is held at voltage V_d with respect to the outer cylinder (and the center cylinder); the local contribution from the narrow gap from the center conductor to the door (as well as the parallel plate contribution of the end of the center conductor to door) are not included in this plot (and must be added). This plot is a comparison of the coaxial Bessel function summation associated with the structure to door capacitve element shown by the black curve with the simple fit for this quantity shown by the gray curve.

3.10 Support Capacitance Element To Outer Cylinder

The center conductor structure has a capacitance to the outer conductor C_{insul}. For a simple coaxial case

$$C_{insul} \approx 2\pi\varepsilon_0 \ell_{coax} / \ln(b/a) \tag{261}$$

However, in some cases there may be direct connections to the cylinder isolated by thin insulator coatings, where the simplest calculation would be

$$C_{insul} = \varepsilon_0 \varepsilon_r A_{insulator} / g_{insulator} \tag{262}$$

where for dielectric coatings isolating the structures, a relative permittivity of ε_r may be present. In either case the center conductor voltage will be the result of a capacitive divider

$$V = \frac{C_{struc}}{C_{stuct} + C_{insul}} V_d \tag{263}$$

4 COAXIAL REGION MAGNETIC FIELDS

The coaxial region has an induced field from the door represented by fields propagating in the higher-order waveguide modes, which decay along the length direction. Because the center conductor is open circuited at both ends the TEM mode for the magnetic field is negligible. The magnetic field is nevertheless important because it directly drives surface currents at the opposing end of the center conductor independent of displacement current coupling (which is negligible at these low frequencies).

4.1 Magnetic Field In Coaxial Region

The quasi-magnetostatic field satisfying

$$\nabla \times \underline{H} = 0 \tag{264}$$

is taken to be represented by the magnetic scalar potential

$$\underline{H} = -\nabla \phi_m \tag{265}$$

Gauss's law

$$\nabla \cdot \underline{B} = \rho_m \tag{266}$$

and constitutive equation (relating magnetic induction $\underline{B}$ to the field $\underline{H}$)

$$\underline{B} = \mu_0 \underline{H} \tag{267}$$

satisfies a Poisson equation

$$\nabla^2 \phi_m = -\rho_m / \mu_0 \tag{268}$$

In regions free of magnetic charge ρ_m this is Laplace's equation

$$\nabla^2 \phi_m = \left(\frac{\partial^2}{\partial \rho^2} + \frac{1}{\rho} \frac{\partial}{\partial \rho} + \frac{1}{\rho^2} \frac{\partial^2}{\partial \varphi^2} + \frac{\partial^2}{\partial z^2} \right) \phi_m = 0 \tag{269}$$

with radial boundary conditions in the coaxial region

$$H_\rho = -\frac{\partial \phi_m}{\partial \rho} = 0 \ , \ \rho = a, b \tag{270}$$

and has solutions

$$\phi_m = \left\{ J'_m \left(\zeta'_{m,n} a \right) Y_m \left(\zeta'_{m,n} \rho \right) - J_m \left(\zeta'_{m,n} \rho \right) Y'_m \left(\zeta'_{m,n} a \right) \right\} \left\{ \begin{array}{c} \cos(m\varphi) \\ \sin(m\varphi) \end{array} \right\} e^{\pm \zeta'_{m,n} z} \tag{271}$$

where

$$J'_m \left(\zeta'_{m,n} a \right) Y'_m \left(\zeta'_{m,n} b \right) - J'_m \left(\zeta'_{m,n} b \right) Y'_m \left(\zeta'_{m,n} a \right) = 0 \tag{272}$$

Note that the Laplace solutions $\rho^{\pm m} (c_0 + c_1 z) \cos(m\varphi)$ and $\rho^{\pm m} (c_0 + c_1 z) \sin(m\varphi)$ cannot be used since such pairs do not obey both the boundary conditions. Some solutions for the symmetric case $m = 0$ are [4]

$$J'_0 \left(\zeta'_{0,n} a \right) Y'_0 \left(\zeta'_{0,n} b \right) - J'_0 \left(\zeta'_{0,n} b \right) Y'_0 \left(\zeta'_{0,n} a \right) = J_1 \left(\zeta'_{0,n} a \right) Y_1 \left(\zeta'_{0,n} b \right) - J_1 \left(\zeta'_{0,n} b \right) Y_1 \left(\zeta'_{0,n} a \right) = 0 \tag{273}$$

$$\zeta'_{0,1}a \approx 2.15647249 \text{ for } a/b = 0.4 \tag{274}$$

$$\zeta'_{0,1}a \approx 4.75805426 \text{ for } a/b = 0.6 \tag{275}$$

$$\zeta'_{0,2}a \approx 4.22309 \text{ for } a/b = 0.4 \tag{276}$$

but we are not primarily interested in this symmetric case. An asymptotic formula is [4]

$$\zeta'_{m,n}a \sim \beta + \frac{p}{\beta} + \frac{q-p^2}{\beta^3} + \frac{r-4pq+2p^3}{\beta^5} + \cdots \tag{277}$$

where

$$\beta = n\pi/\left(b/a-1\right) \tag{278}$$

$$p = \left(4m^2+3\right)/\left(8b/a\right) \tag{279}$$

$$q = \frac{\left(16m^4+184m^2-63\right)\left(b^2/a^2+b/a+1\right)}{6\left(4b/a\right)^3} \tag{280}$$

$$r = \frac{\left(64m^6+2960m^4-8212m^2+1899\right)\left(b^4/a^4+b^3/a^3+b^2/a^2+b/a+1\right)}{5\left(4b/a\right)^5} \tag{281}$$

$$\zeta'_{m,n}a \sim n\pi/\left(b/a-1\right) + \left(4m^2+3\right)\frac{1}{2}\left(\frac{b/a-1}{4n\pi b/a}\right) \tag{282}$$

$$+\left\{\left(16m^4+184m^2-63\right)\left(b^2/a^2+b/a+1\right) - 6\left(4m^2+3\right)^2\left(b/a\right)\right\}\frac{1}{6}\left(\frac{b/a-1}{4n\pi b/a}\right)^3 + \cdots \tag{283}$$

Then

$$\zeta'_{0,1}a \sim \pi/\left(b/a-1\right) + \frac{3}{2}\left(\frac{b/a-1}{4\pi b/a}\right) - \frac{1}{2}\left[21\left(b^2/a^2+1\right)+39b/a\right]\left(\frac{b/a-1}{4\pi b/a}\right)^3$$

$$+\frac{r\left(4b/a\right)^4 - \frac{1}{12}\left(16m^4+184m^2-63\right)\left(b^2/a^2+b/a+1\right)\left(4m^2+3\right)+\left(4m^2+3\right)^3\left(b/a\right)}{\left(4\pi b/a\right)^4\pi/\left(b/a-1\right)^5} + \cdots \tag{284}$$

$$\zeta'_{1,1}a \sim \pi/\left(b/a-1\right) + \frac{7}{2}\left(\frac{b/a-1}{4\pi b/a}\right) + \left\{137\left(b^2/a^2+1\right) - 157b/a\right\}\frac{1}{6}\left(\frac{b/a-1}{4\pi b/a}\right)^3 + \cdots \tag{285}$$

$$\zeta'_{2,1}a \sim \pi/\left(b/a-1\right) + \frac{19}{2}\left(\frac{b/a-1}{4\pi b/a}\right) + \left\{929\left(b^2/a^2+1\right) - 1237\left(b/a\right)\right\}\frac{1}{6}\left(\frac{b/a-1}{4\pi b/a}\right)^3 + \cdots \tag{286}$$

$$\zeta'_{3,1}a \sim \pi/\left(b/a-1\right) + \frac{39}{2}\left(\frac{b/a-1}{4\pi b/a}\right) + \left\{963\left(b^2/a^2+1\right) - 2079\left(b/a\right)\right\}\frac{1}{2}\left(\frac{b/a-1}{4\pi b/a}\right)^3 + \cdots \tag{287}$$

For the example $a/b = 0.4$

$$\zeta'_{0,1}a \sim \frac{2}{3}\pi + \frac{3}{2}\left(\frac{3}{20\pi}\right) - \frac{999}{8}\left(\frac{3}{20\pi}\right)^3 + \cdots$$

$$\sim \frac{2}{3}\pi\left[1 + \frac{3}{20}\left(\frac{3}{2\pi}\right)^2 - \frac{999}{8000}\left(\frac{3}{2\pi}\right)^4 + \cdots\right] \approx \frac{2}{3}\pi\left[1 + 0.0341959 - 0.0064899455 + \cdots\right]$$

$$\approx 2.1524223 \tag{288}$$

$$\zeta'_{1,1}a \sim \frac{2}{3}\pi + \frac{7}{2}\left(\frac{3}{20\pi}\right) + \frac{801}{8}\left(\frac{3}{20\pi}\right)^3 + \cdots$$

$$\sim \frac{2}{3}\pi\left[1 + \frac{7}{20}\left(\frac{3}{2\pi}\right)^2 + \frac{801}{8000}\left(\frac{3}{2\pi}\right)^4 + \cdots\right] \approx \frac{2}{3}\pi\left[1 + 0.079790432 + 0.005203650 + \cdots\right]$$

$$\approx 2.2724063 \tag{289}$$

$$\zeta'_{2,1} \sim \frac{2}{3}\pi + \frac{19}{2}\left(\frac{3}{20\pi}\right) + \frac{1}{8}4857\left(\frac{3}{20\pi}\right)^3 + \cdots$$

$$\sim \frac{2}{3}\pi\left[1 + \frac{19}{20}\left(\frac{3}{2\pi}\right)^2 + \frac{1}{8000}4857\left(\frac{3}{2\pi}\right)^4 + \cdots\right] \approx \frac{2}{3}\pi\left[1 + 0.21657403 + 0.0316 + \cdots\right]$$

$$\approx 2.6141 \tag{290}$$

$$\zeta'_{3,1}a \sim \frac{2}{3}\pi + \frac{39}{2}\left(\frac{3}{20\pi}\right) + \frac{1}{8}7137\left(\frac{3}{20\pi}\right)^3 + \cdots$$

$$\sim \frac{2}{3}\pi\left[1 + \frac{39}{20}\left(\frac{3}{2\pi}\right)^2 + \frac{7137}{8000}\left(\frac{3}{2\pi}\right)^4 + \cdots\right] \approx \frac{2}{3}\pi\left[1 + 0.4445 + 0.0464 + \cdots\right]$$

$$\approx 3.1226 \tag{291}$$

As n increases these results increase nearly proportional to n. If the structure is open circuited beyond some point $z = 0$, the TEM mode is driven to zero beyond this point (at low frequencies where the displacement current is negligible) but the higher-order modes continue with decay. The lowest order asymmetric $m = 1$ mode has roots of the equation [4]

$$J'_1\left(\zeta'_{1,n}a\right)Y'_1\left(\zeta'_{1,n}b\right) - J'_1\left(\zeta'_{1,n}b\right)Y'_1\left(\zeta'_{1,n}a\right) = 0$$

$$= \left[J_0\left(\zeta'_{1,n}a\right) - \frac{1}{\zeta'_{1,n}a}J_1\left(\zeta'_{n,1}a\right)\right]\left[Y_0\left(\zeta'_{1,n}b\right) - \frac{1}{\zeta'_{1,n}b}Y_1\left(\zeta'_{1,n}b\right)\right]$$

$$- \left[J_0\left(\zeta'_{1,n}b\right) - \frac{1}{\zeta'_{1,n}b}J_1\left(\zeta'_{1,n}b\right)\right]\left[Y_0\left(\zeta'_{1,n}a\right) - \frac{1}{\zeta'_{1,n}a}Y_1\left(\zeta'_{1,n}a\right)\right]$$

$$= \left[J_0\left(\zeta'_{1,n}a\right)Y_0\left(\zeta'_{1,n}b\right) - J_0\left(\zeta'_{1,n}b\right)Y_0\left(\zeta'_{1,n}a\right)\right]$$

$$-\frac{1}{\zeta'_{1,n}b}\left[J_0\left(\zeta'_{1,n}a\right)Y_1\left(\zeta'_{1,n}b\right) - J_1\left(\zeta'_{1,n}b\right)Y_0\left(\zeta'_{1,n}a\right)\right]$$

$$-\frac{1}{\zeta'_{1,n}a}\left[J_1\left(\zeta'_{1,n}a\right)Y_0\left(\zeta'_{1,n}b\right) - J_0\left(\zeta'_{1,n}b\right)Y_1\left(\zeta'_{1,n}a\right)\right]$$

$$+\frac{1}{\zeta'_{1,n}a\zeta'_{1,n}b}\left[J_1\left(\zeta'_{1,n}a\right)Y_1\left(\zeta'_{1,n}b\right) - J_1\left(\zeta'_{1,n}b\right)Y_1\left(\zeta'_{1,n}a\right)\right] \tag{292}$$

with asymptotic solution

$$\zeta'_{1,n}a \sim \beta + \frac{p}{\beta} + \frac{q-p^2}{\beta^3} + \frac{r-4pq+2p^3}{\beta^5} + \cdots \tag{293}$$

where

$$\beta = n\pi/\left(b/a-1\right) \tag{294}$$

$$p = 7/\left(8b/a\right) \tag{295}$$

$$q = \frac{137\left(b^2/a^2 + b/a + 1\right)}{6\left(4b/a\right)^3} \tag{296}$$

$$r = \frac{-3289\left(b^4/a^4 + b^3/a^3 + b^2/a^2 + b/a + 1\right)}{5\left(4b/a\right)^5} \tag{297}$$

$$\zeta'_{1,n}a \sim n\pi/\left(b/a-1\right) + \frac{7}{2}\left(\frac{b/a-1}{4n\pi b/a}\right) + \left\{137\left(b^2/a^2+1\right) - 157\left(b/a\right)\right\}\frac{1}{6}\left(\frac{b/a-1}{4n\pi b/a}\right)^3 + \cdots \tag{298}$$

$$\zeta'_{1,1}a \sim \pi/\left(b/a-1\right) + \frac{7}{2}\left(\frac{b/a-1}{4\pi b/a}\right) + \left\{137\left(b^2/a^2+1\right) - 157b/a\right\}\frac{1}{6}\left(\frac{b/a-1}{4\pi b/a}\right)^3 + \cdots \tag{299}$$

$$\zeta'_{1,2}a \sim 2\pi/\left(b/a-1\right) + \frac{7}{4}\left(\frac{b/a-1}{4\pi b/a}\right) + \left\{137\left(b^2/a^2+1\right) - 157\left(b/a\right)\right\}\frac{1}{48}\left(\frac{b/a-1}{4\pi b/a}\right)^3 + \cdots \tag{300}$$

However, the first (or initial) root is not captured by this asymptotic formula (and we label it with number $n = 0$). We can estimate this particular initial root by examining the physical problem it corresponds to. If we consider a planar waveguide wrapped around the coax at the effective radius ρ_e, the scalar potential can be taken as

$$\nabla^2\phi_m = \left(\frac{\partial^2}{\partial x^2} + \frac{\partial^2}{\partial z^2}\right)\phi_m = 0 \tag{301}$$

with

$$\frac{\partial \phi_m}{\partial \rho} = \frac{\partial \phi_m}{\partial y} = 0 \ , \ \rho = a, b \tag{302}$$

$$\phi_m = e^{\pm \zeta'_{1,n} z} \left\{ \begin{array}{c} \cos\left(\zeta'_{1,0} x\right) \\ \sin\left(\zeta'_{1,0} x\right) \end{array} \right\} \tag{303}$$

$$\phi_m \left(x = 0\right) = \phi_m \left(x = 2\pi\rho_e\right) \tag{304}$$

$$\rho_e = \left(a + b\right)/2 \tag{305}$$

$$\zeta'_{1,0} 2\pi\rho_e = 2\pi \tag{306}$$

$$\zeta'_{1,0} \rho_e = 1 \tag{307}$$

$$\zeta'_{1,0} b \sim 2/\left(1 + a/b\right) \tag{308}$$

The numerical roots are

a/b	$\zeta'_{1,0}b$	$\zeta'_{1,1}b$	$\zeta'_{1,2}b$	$\zeta'_{1,3}b$	$\zeta'_{1,4}b$	$\zeta'_{1,5}b$	$\zeta'_{1,6}b$
0.1	1.8034701	5.1371365	8.1991623	11.358793	14.634361	17.986417	21.383688
0.2	1.7051157	4.9608548	8.4330686	12.165052	15.993233	19.861628	23.750000
0.3	1.5820647	5.1373946	9.3082665	13.683644	18.115878	22.570710	27.036720
0.4	1.4617819	5.6591042	10.683252	15.848084	21.048785	26.263701	31.485678
0.5	1.3546720	6.5649424	12.706422	18.942659	25.202487	31.471691	37.745567
0.6	1.2620756	8.0410875	15.801059	23.623919	31.462382	39.307062	47.154847
0.7	1.1823634	10.591835	21.003708	31.455738	41.917753	52.383756	62.851750
0.8	1.1133663	15.777712	31.450758	47.147105	62.849263	78.553743	94.259385
0.9	1.0531161	31.446885	62.847328	94.258096	125.67144	157.08582	188.50072

The approximate roots are (the asymptotic expression for $n \geq 1$ is evaluated to three terms except the value with two terms is shown for some of the first roots and the second column is the physical planar waveguide approximation for the $n = 0$ root)

a/b	$2b/\left(a+b\right)$	$\sim \zeta'_{1,1}b$	$\sim \zeta'_{1,2}b$	$\sim \zeta'_{1,3}b$	$\sim \zeta'_{1,4}b$	$\sim \zeta'_{1,5}b$	$\sim \zeta'_{1,6}b$
0.1	1.8181818	5.9973489_2 (13.508129)	8.2346622_2 (9.1735097)	11.307539_2 (11.585716)	14.589307_2 (14.706663)	18.014717	21.396505
0.2	1.6666667	5.0410754_2 (5.6381588)	8.4110239_2 (8.4856594)	12.174448	15.995814	19.862548	23.750390
0.3	1.5384615	5.1378722_2 (5.2469479)	9.3145548	13.684636	18.116133	22.570797	27.036756
0.4	1.4285714	5.6810157	10.684272	15.848233	21.048822	26.263713	31.485683
0.5	1.3333333	6.5694964	12.706605	18.942685	25.202493	31.471693	37.745568
0.6	1.25	8.0419548	15.801090	23.623923	31.462383	39.307063	47.154847
0.7	1.1764706	10.591965	21.003712	31.455738	41.917753	52.383756	62.851750
0.8	1.1111111	15.777724	31.450758	47.147105	62.849263	78.553743	94.259385
0.9	1.0526316	31.446886	62.847328	94.258096	125.67144	157.08582	188.50072

4.2 Magnetic Field In Cylindrical Region

The cylindrical region has the Laplace equation

$$\nabla^2\phi_m = 0 = \left(\frac{\partial^2}{\partial\rho^2} + \frac{1}{\rho}\frac{\partial}{\partial\rho} + \frac{1}{\rho^2}\frac{\partial^2}{\partial\varphi^2} + \frac{\partial^2}{\partial z^2}\right)\phi_m \tag{309}$$

with radial boundary condition

$$\frac{\partial\phi_m}{\partial\rho}(\rho = b) = 0 \tag{310}$$

we take the solution as

$$\phi_m = J_m\left(j'_{m,n}\rho/b\right)e^{\pm j'_{m,n}z/b}\left\{\begin{array}{c}\cos(m\varphi)\\ \sin(m\varphi)\end{array}\right\} \tag{311}$$

where

$$J'_m\left(j'_{m,n}\right) = 0 \tag{312}$$

The first roots now being

n	$j'_{0,n}$	$j'_{1,n}$	$j'_{2,n}$
1	0	1.84118	3.05424
2	3.83170	5.33144	6.70613
3	7.01559	8.53632	9.96947
4	10.17346	11.70600	13.17037
5	13.32369	14.86359	16.34752

4.3 Magnetic Field Coaxial Region Mode Excitation

The excitation of the coaxial region modes from the door slot is examined without and with a conductive door gasket.

4.3.1 No Conductive Gasket Coaxial Region Mode Excitation

If no conductive gasket exists then as a worst case we take the return to occur on the opposite side of the slot from the strike point (through the hinge connection or through a breakdown) and then the current distribution on the door side of the slot is

$$I(s) = \pm\frac{1}{2}I_0(t) = \frac{1}{2}I_0(t)\,\mathrm{sgn}(s)\ ,\quad -h < s < h \tag{313}$$

$$2h = 2\pi b \tag{314}$$

Let us first consider a semi-infinite coax with magnetic flux per unit length $\Phi(s)$ injected at $z = 0$ around the circumference with $\rho = b$ and $s = b\varphi$. The magnetic flux per unit length through the slot is then (there may be some contribution from the magnetic field penetrating the metal, however for larger slot widths with metallic walls, this is probably small at earlier times)

$$q_m = \Phi(s) = LI(s) = LI_0(t)\,\mathrm{sgn}(s) = q_{m0}\mathrm{sgn}(\varphi) \tag{315}$$

$$L \approx \mu_0 w/d \tag{316}$$

and note the Fourier expansion

$$\mathrm{sgn}\left(\varphi\right)=\frac{4}{\pi}\sum_{m,odd}\frac{\sin\left(m\varphi\right)}{m} \tag{317}$$

In this section we find the magnetic charge per unit length assuming the potential and fields will be found with the conducting boundaries taken into account; in other words, there is no doubling of the magnetic charge imposed, as there often is when aperture dipole moments are defined on a ground plane (see section on hole penetration below). From Laplace's equation on the interior of the cylinder

$$\nabla^2\phi_m=0=\left(\frac{\partial^2}{\partial\rho^2}+\frac{1}{\rho}\frac{\partial}{\partial\rho}+\frac{1}{\rho^2}\frac{\partial^2}{\partial\varphi^2}+\frac{\partial^2}{\partial z^2}\right)\phi_m \tag{318}$$

we take the solution as

$$\phi_m=R_m\left(\zeta'_{m,n}\rho\right)\left\{\begin{array}{c}\cos\left(m\varphi\right)\\ \sin\left(m\varphi\right)\end{array}\right\}e^{\pm\zeta'_{m,n}z} \tag{319}$$

where

$$R_m\left(\zeta'_{m,n}\rho\right)=J'_m\left(\zeta'_{m,n}a\right)Y_m\left(\zeta'_{m,n}\rho\right)-J_m\left(\zeta'_{m,n}\rho\right)Y'_m\left(\zeta'_{m,n}a\right) \tag{320}$$

and from the radial coaxial boundary conditions

$$R'_m\left(\zeta'_{n,m}\rho\right)=J'_m\left(\zeta'_{m,n}a\right)Y'_m\left(\zeta'_{m,n}\rho\right)-J'_m\left(\zeta'_{m,n}\rho\right)Y'_m\left(\zeta'_{m,n}a\right)=0\ ,\ \rho=a,b \tag{321}$$

Also by use of the Wronskian for Bessel functions

$$R_m\left(\zeta'_{m,n}a\right)=J'_m\left(\zeta'_{m,n}a\right)Y_m\left(\zeta'_{m,n}a\right)-J_m\left(\zeta'_{m,n}a\right)Y'_m\left(\zeta'_{m,n}a\right)=-W\left[J_m\left(\zeta'_{m,n}a\right),Y_m\left(\zeta'_{m,n}a\right)\right]=-\frac{2}{\pi\zeta'_{m,n}a} \tag{322}$$

The orthogonality relation is

$$\begin{aligned}\int_a^b R_m\left(\zeta'_{m,n}\rho\right)R_m\left(\zeta'_{m,n'}\rho\right)\rho d\rho&=\delta_{nn'}\left[\frac{1}{2}\rho^2\left(1-\frac{m^2}{\zeta'^2_{m,n}\rho^2}\right)R_m^2\left(\zeta'_{m,n}\rho\right)+R'^2_m\left(\zeta'_{m,n}\rho\right)\right]_a^b\\&=\delta_{nn'}\left[\frac{1}{2}b^2\left(1-\frac{m^2}{\zeta'^2_{m,n}b^2}\right)R_m^2\left(\zeta'_{m,n}b\right)-\left(1-\frac{m^2}{\zeta'^2_{m,n}a^2}\right)\frac{2}{\pi^2\zeta'^2_{m,n}}\right]\end{aligned} \tag{323}$$

The axial field boundary condition is taken as

$$\mu_0H_z\left(\rho,\varphi,z=0\right)=\delta\left(\rho-b\right)q_{m0}\mathrm{sgn}\left(\varphi\right)=\delta\left(\rho-b\right)q_{m0}\frac{4}{\pi}\sum_{m,odd}\frac{\sin\left(m\varphi\right)}{m} \tag{324}$$

The potential is then expanded as

$$\phi_m=\sum_n\sum_m A_{m,n}R_m\left(\zeta'_{m,n}\rho\right)\sin\left(m\varphi\right)e^{-\zeta'_{m,n}z} \tag{325}$$

Taking

$$A_{m,n} = \widetilde{A}_{m,n} \frac{4}{\mu_0 \pi m \zeta'_{m,n}} q_{m0} \ , \ m \text{ odd} \tag{326}$$

$$\phi_m = (q_{m0}/\mu_0) \sum_n \frac{4}{\pi} \sum_{m,odd} \widetilde{A}_{m,n} \frac{1}{\zeta'_{m,n}} R_m \left(\zeta'_{m,n}\rho\right) \frac{\sin(m\varphi)}{m} e^{-\zeta'_{m,n}z} \tag{327}$$

and

$$\sum_n \sum_{m,odd} \widetilde{A}_{m,n} R_m \left(\zeta'_{m,n}\rho\right) \frac{\sin(m\varphi)}{m} = \delta(\rho - b) \sum_{m,odd} \frac{\sin(m\varphi)}{m} \tag{328}$$

Using orthogonality

$$\sum_n \sum_{m,odd} \widetilde{A}_{m,n} \frac{\sin(m\varphi)}{m} \int_a^b R_m \left(\zeta'_{m,n}\rho\right) R_m \left(\zeta'_{m,n'}\rho\right) \rho d\rho = \sum_{m,odd} \frac{\sin(m\varphi)}{m} \int_a^b R_m \left(\zeta'_{m,n'}\rho\right) \delta(\rho - b) \rho d\rho \tag{329}$$

or

$$\sum_{m,odd} \widetilde{A}_{m,n} \frac{\sin(m\varphi)}{m} \left[\frac{1}{2} b^2 \left(1 - \frac{m^2}{\zeta'^2_{m,n} b^2}\right) R_m^2 \left(\zeta'_{m,n} b\right) - \left(1 - \frac{m^2}{\zeta'^2_{m,n} a^2}\right) \frac{2}{\pi^2 \zeta'^2_{m,n}}\right] = \sum_{m,odd} \frac{\sin(m\varphi)}{m} b R_m \left(\zeta'_{m,n} b\right) \tag{330}$$

or

$$\widetilde{A}_{m,n} \left[\frac{1}{2} b^2 \left(1 - \frac{m^2}{\zeta'^2_{m,n} b^2}\right) R_m^2 \left(\zeta'_{m,n} b\right) - \left(1 - \frac{m^2}{\zeta'^2_{m,n} a^2}\right) \frac{2}{\pi^2 \zeta'^2_{m,n}}\right] = b R_m \left(\zeta'_{m,n} b\right) \tag{331}$$

Now for a sizable distance down the coax we can truncate at the $m = 1$, $n = 0$ term

$$\phi_m \sim (q_{m0}/\mu_0) \frac{4}{\pi} \widetilde{A}_{1,0} \frac{1}{\zeta'_{1,0}} R_1 \left(\zeta'_{1,0}\rho\right) \sin(\varphi) e^{-\zeta'_{1,0}z} \tag{332}$$

$$\widetilde{A}_{1,0} \left[\left(1 - \frac{1}{\zeta'^2_{1,0} b^2}\right) R_1^2 \left(\zeta'_{1,0} b\right) - \left(1 - \frac{1}{\zeta'^2_{1,0} a^2}\right) \frac{4}{\pi^2 \zeta'^2_{1,0} b^2}\right] = 2 R_1 \left(\zeta'_{1,0} b\right) / b \tag{333}$$

or

$$\phi_m \sim 4 (q_{m0}/\mu_0) \frac{\frac{2}{\pi \zeta'_{1,0} b} R_1 \left(\zeta'_{1,0} b\right)}{\left(1 - \frac{1}{\zeta'^2_{1,0} b^2}\right) R_1^2 \left(\zeta'_{1,0} b\right) - \left(1 - \frac{1}{\zeta'^2_{1,0} a^2}\right) \frac{4}{\pi^2 \zeta'^2_{1,0} b^2}} R_1 \left(\zeta'_{1,0}\rho\right) \sin(\varphi) e^{-\zeta'_{1,0}z} \tag{334}$$

$$R_m \left(\zeta'_{m,n}\rho\right) = J'_m \left(\zeta'_{m,n} a\right) Y_m \left(\zeta'_{m,n}\rho\right) - J_m \left(\zeta'_{m,n}\rho\right) Y'_m \left(\zeta'_{m,n} a\right) \tag{335}$$

where the lowest mode root is our planar waveguide approximation

$$\zeta'_{1,0} \sim 2/(b + a) \tag{336}$$

4.3.2 Conductive Gasket Coaxial Region Mode Excitation

When a conductive gasket is present the slot current becomes the lossy transmission line similarity solution

$$I(s,t) = Ati^2\mathrm{erfc}(u) = At\left[\frac{1}{2}\left(\frac{1}{2}+\frac{1}{4}s^2LG/t\right)\mathrm{erfc}\left(\frac{1}{2}s\sqrt{LG/t}\right) - \frac{1}{4}s\sqrt{LG/t}\frac{1}{\sqrt{\pi}}e^{-\frac{1}{4}s^2LG/t}\right] \tag{337}$$

where the constant A is determined from I_0 by means of

$$I(0,t) = At/4 = \frac{1}{2}\left(I_0/\tau_r\right)t \tag{338}$$

$$q_m(s) = \Phi(s) = LI(s) \tag{339}$$

The axial field boundary condition is

$$\mu_0 H_z(\rho,\varphi,z=0) = \delta(\rho-b)\,q_m(s) \tag{340}$$

The potential expansion

$$\phi_m = \sum_n\sum_m A_{m,n}R_m\left(\zeta'_{m,n}\rho\right)\sin(m\varphi)\,e^{-\zeta'_{m,n}z} \tag{341}$$

then gives

$$\delta(\rho-b)\,q_m(s) = \mu_0 H_z(\rho,\varphi,z=0) = -\mu_0\frac{\partial}{\partial z}\phi_m = \mu_0\sum_n\sum_m A_{m,n}\zeta'_{m,n}R_m\left(\zeta'_{m,n}\rho\right)\sin(m\varphi) \tag{342}$$

Using the orthogonality relations

$$\int_0^\pi \sin(m\varphi)\sin(m'\varphi)\,d\varphi = \frac{1}{2}\int_0^\pi\left[\cos(m-m')\varphi - \cos(m+m')\varphi\right]d\varphi = \frac{1}{2}\left[\frac{\sin(m-m')\varphi}{(m-m')} - \frac{\sin(m+m')\varphi}{(m+m')}\right]_0^\pi = \frac{\pi}{2}\delta_{mm'} \tag{343}$$

$$\begin{aligned}\int_a^b R_m\left(\zeta'_{m,n}\rho\right)R_m\left(\zeta'_{m,n'}\rho\right)\rho d\rho &= \delta_{nn'}\left[\frac{1}{2}\rho^2\left(1-\frac{m^2}{\zeta'^2_{m,n}\rho^2}\right)R_m^2\left(\zeta'_{m,n}\rho\right) + R_m'^2\left(\zeta'_{m,n}\rho\right)\right]_a^b \\ &= \delta_{nn'}\left[\frac{1}{2}b^2\left(1-\frac{m^2}{\zeta'^2_{m,n}b^2}\right)R_m^2\left(\zeta'_{m,n}b\right) - \left(1-\frac{m^2}{\zeta'^2_{m,n}a^2}\right)\frac{2}{\pi^2\zeta'^2_{m,n}}\right]\end{aligned} \tag{344}$$

we can write

$$R_m\left(\zeta'_{m,n}b\right)\int_0^\pi \sin(m\varphi)\,q_m(b\varphi)\,bd\varphi = \mu_0\frac{\pi}{2}A_{m,n}\zeta'_{m,n}\left[\frac{1}{2}b^2\left(1-\frac{m^2}{\zeta'^2_{m,n}b^2}\right)R_m^2\left(\zeta'_{m,n}b\right) - \left(1-\frac{m^2}{\zeta'^2_{m,n}a^2}\right)\frac{2}{\pi^2\zeta'^2_{m,n}}\right] \tag{345}$$

In the case where the decay length along the gasket is much smaller than the radius of the door slot we can approximate by replacing the sine by its argument

$$\frac{1}{b}R_1\left(\zeta'_{1,n}b\right)\int_0^\infty sq_m\left(s\right)ds=\mu_0\frac{\pi}{2}A_{1,n}\zeta'_{1,n}\left[\frac{1}{2}b^2\left(1-\frac{1}{\zeta'^2_{1,n}b^2}\right)R_1^2\left(\zeta'_{1,n}b\right)-\left(1-\frac{1}{\zeta'^2_{1,n}a^2}\right)\frac{2}{\pi^2\zeta'^2_{1,n}}\right] \tag{346}$$

Noting that

$$\int_0^\infty sq_m\left(s\right)ds=L\int_0^\infty sI\left(s,t\right)ds=\frac{4At^2}{G}\int_0^\infty i^2\mathrm{erfc}\left(u\right)udu \tag{347}$$

where

$$I\left(s,t\right)=Ati^2\mathrm{erfc}\left(u\right)=2\left(I_0/\tau_r\right)ti^2\mathrm{erfc}\left(u\right) \tag{348}$$

$$u=\frac{1}{2}s\sqrt{LG/t} \tag{349}$$

integration by parts allows us to write

$$\int_u^\infty i^2\mathrm{erfc}\left(u\right)udu=\left[-i^3\mathrm{erfc}\left(u\right)u\right]_u^\infty+\int_u^\infty i^3\mathrm{erfc}\left(u\right)du=i^3\mathrm{erfc}\left(u\right)u+i^4\mathrm{erfc}\left(u\right) \tag{350}$$

where

$$i^n\mathrm{erfc}\left(u\right)=\int_u^\infty i^{n-1}\mathrm{erfc}\left(u'\right)du' \tag{351}$$

and

$$\lim_{u\to0}i^n\mathrm{erfc}\left(u\right)=\frac{1}{2^n\Gamma\left(n/2+1\right)} \tag{352}$$

yields

$$\int_0^\infty i^2\mathrm{erfc}\left(u\right)udu=\lim_{u\to0}i^4\mathrm{erfc}\left(u\right)=\frac{1}{32} \tag{353}$$

$$\frac{1}{b}R_1\left(\zeta'_{1,n}b\right)\frac{\left(I_0/\tau_r\right)t^2}{4G}=\mu_0\frac{\pi}{2}A_{1,n}\zeta'_{1,n}\left[\frac{1}{2}b^2\left(1-\frac{1}{\zeta'^2_{1,n}b^2}\right)R_1^2\left(\zeta'_{1,n}b\right)-\left(1-\frac{1}{\zeta'^2_{1,n}a^2}\right)\frac{2}{\pi^2\zeta'^2_{1,n}}\right] \tag{354}$$

The growth of the coefficient with $O\left(t^2\right)$ results from the increasing current level in addition to the increasing decay length with time. This behavior fails as we leave the linear growth regime of the current.

To address the region of slowly decaying current near the peak value we take $\beta=0$ to obtain a constant current behavior at $s=0=u$

$$I\left(s,t\right)=\frac{1}{2}I_0\mathrm{erfc}\left(u\right) \tag{355}$$

$$u=\frac{1}{2}s\sqrt{LG/t} \tag{356}$$

Then

$$\int_0^\infty sq_m(s)\,ds = L\int_0^\infty sI(s,t)\,ds = \frac{2I_0t}{G}\int_0^\infty \mathrm{erfc}(u)\,udu \tag{357}$$

$$\int_u^\infty \mathrm{erfc}(u)\,udu = \left[-i\mathrm{erfc}(u)\,u\right]_u^\infty + \int_u^\infty i\mathrm{erfc}(u)\,du = i\mathrm{erfc}(u)\,u + i^2\mathrm{erfc}(u) \tag{358}$$

$$\int_0^\infty \mathrm{erfc}(u)\,udu = \lim_{u\to 0} i^2\mathrm{erfc}(u) = 1/4 \tag{359}$$

and thus we find the coefficient as

$$\frac{1}{b}R_1\left(\zeta'_{1,n}b\right)\frac{I_0t}{2G} = \mu_0\frac{\pi}{2}A_{1,n}\zeta'_{1,n}\left[\frac{1}{2}b^2\left(1-\frac{1}{\zeta'^2_{1,n}b^2}\right)R_1^2\left(\zeta'_{1,n}b\right) - \left(1-\frac{1}{\zeta'^2_{1,n}a^2}\right)\frac{2}{\pi^2\zeta'^2_{1,n}}\right] \tag{360}$$

This form gives us what we are after. We want to maximize the derivative of the magnetic field on the coaxial structure. Notice that the time derivative of this coefficient and the time derivative of the preceding form for this coefficient match at $t=\tau_r$. Because this new form for the coefficient is linear in time it produces a constant time derivative after the rise time portion of the current. It is only valid, however, during the period where the decay length is smaller than the radius of the slot structure.

Taking only the leading term of the coaxial potential $n=0$

$$\phi_m \sim A_{1,0}R_1\left(\zeta'_{1,0}\rho\right)\sin(\varphi)\,e^{-\zeta'_{1,0}z} \tag{361}$$

$$\frac{1}{b}R_1\left(\zeta'_{1,0}b\right)\frac{I_0t}{2G} = \mu_0\frac{\pi}{2}A_{1,0}\zeta'_{1,0}\left[\frac{1}{2}b^2\left(1-\frac{1}{\zeta'^2_{1,0}b^2}\right)R_1^2\left(\zeta'_{1,0}b\right) - \left(1-\frac{1}{\zeta'^2_{1,0}a^2}\right)\frac{2}{\pi^2\zeta'^2_{1,0}}\right] \tag{362}$$

We can compare the modal size of this leading mode result with conductive gasket present

$$K_z(\varphi,z) = H_\varphi^{LM}(a,\varphi,z) = -\frac{1}{a}\frac{\partial\phi_m}{\partial\varphi}(a,\varphi,z) \sim -\frac{1}{a}A_{1,0}R_1\left(\zeta'_{1,0}a\right)\cos(\varphi)\,e^{-\zeta'_{1,0}z}$$

$$\sim \frac{I_0t}{b^2G\mu_0}\frac{\frac{4}{\pi^2\zeta'^2_{1,0}a^2b}R_1\left(\zeta'_{1,0}b\right)}{\left(1-\frac{1}{\zeta'^2_{1,0}b^2}\right)R_1^2\left(\zeta'_{1,0}b\right) - \left(1-\frac{1}{\zeta'^2_{1,0}a^2}\right)\frac{4}{\pi^2\zeta'^2_{1,0}b^2}}\cos(\varphi)\,e^{-\zeta'_{1,0}z} \tag{363}$$

to the case without a conductive gasket present. Using the result without a gasket in the following sections, we see that the ratio of the leading modal amplitude with and without gasket is

$$H_\varphi^{LMgas}(a,\varphi,z)/H_\varphi^{LM}(a,\varphi,z) = \frac{I_0t}{2G\mu_0}/\left[4\left(q_{m0}/\mu_0\right)\right] = \frac{I_0t}{b^2G\mu_0}/\left[4LI_0(t)/\mu_0\right]$$

$$= \frac{I_0t}{b^2G\mu_0}/\left[4\left(Lt\left(I_0/\tau_r\right)/\mu_0\right)\right] = \frac{\tau_r}{4b^2LG} \approx \frac{d/d_g}{(2b)^2\sigma_g\left(\mu_0/\tau_r\right)} \tag{364}$$

This ratio is typically very small and is nearly the same as the average voltage ratio in the electric case.

4.4 Maximum Magnetic Field On Center Conductor

We need the magnetic field at the end of the terminated inner conductor to drive a connector. We believe that the current density on the inner cylinder can be used as an estimate of the current density at the center of the end cap of the open circuited center conductor termination in a similar manner to the electric field case (see actual tip field (181) versus maximum center conductor field (182)). This current density or magnetic field is given by

$$K_z(\varphi,z)=H_\varphi^{LM}(a,\varphi,z)=-\frac{1}{a}\frac{\partial\phi_m}{\partial\varphi}(a,\varphi,z)$$

$$\sim 4(q_{m0}/\mu_0)\frac{\frac{4}{\pi^2\zeta_{1,0}'^2a^2b}R_1\left(\zeta_{1,0}'b\right)}{\left(1-\frac{1}{\zeta_{1,0}'^2b^2}\right)R_1^2\left(\zeta_{1,0}'b\right)-\left(1-\frac{1}{\zeta_{1,0}'^2a^2}\right)\frac{4}{\pi^2\zeta_{1,0}'^2b^2}}\cos(\varphi)\,e^{-\zeta_{1,0}'z} \tag{365}$$

If we take position $z=z_1$ and $\varphi=0$

$$(b-a)K_z(0,z_1)\,e^{\zeta_{1,0}'z_1}/\{4(q_{m0}/\mu_0)\}=\frac{(b/a-1)(b/a)\frac{4/\pi^2}{\zeta_{1,0}'^2b^2}R_1\left(\zeta_{1,0}'b\right)}{\left(1-\frac{1}{\zeta_{1,0}'^2b^2}\right)R_1^2\left(\zeta_{1,0}'b\right)-\left(1-\frac{1}{\zeta_{1,0}'^2a^2}\right)\frac{4/\pi^2}{\zeta_{1,0}'^2b^2}} \tag{366}$$

This current density is now applied to the connector at the tip

$$K_{sc}^{cap}\le K_z(0,z_1) \tag{367}$$

which is shown in Figure 4.

4.5 Magnetic Charge At Termination Of Center Conductor

As a check on the preceding approximate estimate of the magnetic field at the open end of the coax, we use matching at the junction between the coaxial and cylindrical regions to estimate the actual tip magnetic field. Note that we are actually ultimately interested in twice the tip magnetic field to represent the magnetic field at the base of the connector (this factor of two is due to the field at the terminated end of the center conductor then impinging on the cylindrical connector, with the maximum value doubling as in a field impinging on a cylinder).

We insert a magnetic surface charge at $z=z_1$

$$\sigma_m(\rho,\varphi,z_1\pm 0)=\pm\mu_0H_z(\rho,\varphi,z_1\pm 0)=\sigma_{m0}(\rho)\sin(\varphi) \tag{368}$$

$$\sigma_{m0}(\rho)=\pm\mu_0H_z(\rho,\pi/2,z_1) \tag{369}$$

The magnetic potential representation in the cylindrical region is

$$\phi_m=(q_{m0}/\mu_0)\frac{4}{\pi}\sin(\varphi)\sum_{n=1}^{\infty}A_{+n}e^{-j_{1,n}'(z-z_1)/b}J_1\left(j_{1,n}'\rho/b\right)\ ,\ z>z_1 \tag{370}$$

and in the coaxial region is

$$\phi_m=\phi_m^{inc}+(q_{m0}/\mu_0)\frac{4}{\pi}\sin(\varphi)\sum_{n=0}^{\infty}A_{-n}e^{-\zeta_{1,n}'(z_1-z)}R_1\left(\zeta_{1,n}'\rho\right)\ ,\ z<z_1 \tag{371}$$

where the problem is driven by an incident lowest order coaxial mode

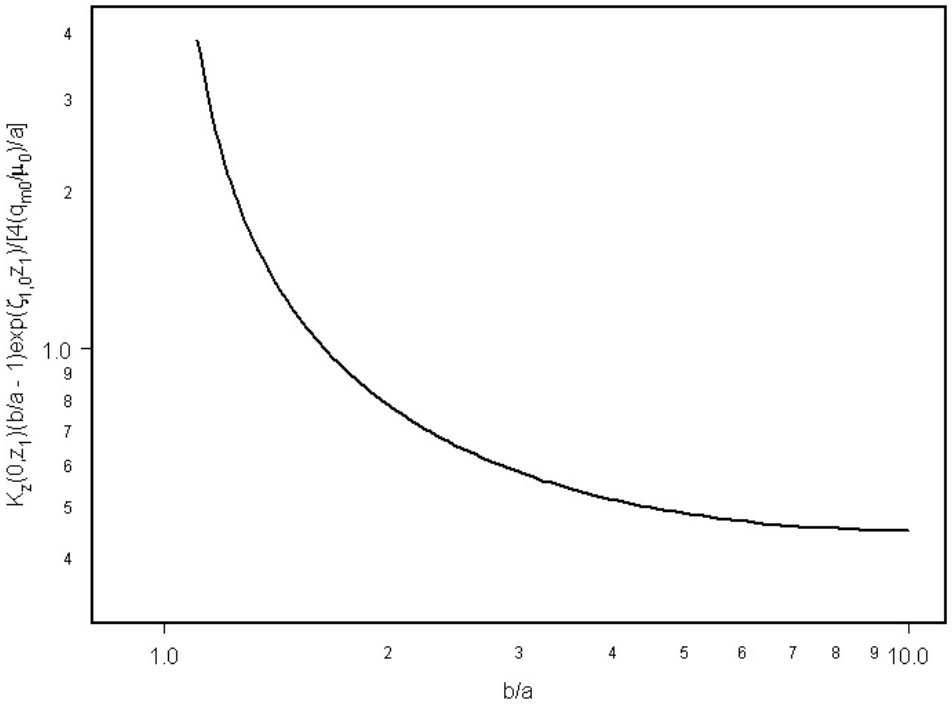

Figure 4: Maximum (as function of azimuth) axial current density of dominant coaxial magnetic mode as a function of coaxial outer-to-inner radii. This can be used as an approximate estimate for the maximum magnetic field (current density) at the tip of the terminating center conductor.

$$\phi_m^{inc} \sim 4\left(q_{m0}/\mu_0\right)\frac{\frac{2}{\pi\zeta'_{1,0}b}R_1\left(\zeta'_{1,0}b\right)}{\left(1-\frac{1}{\zeta'^2_{1,0}b^2}\right)R_1^2\left(\zeta'_{1,0}b\right)-\left(1-\frac{1}{\zeta'^2_{1,0}a^2}\right)\frac{4}{\pi^2\zeta'^2_{1,0}b^2}}R_1\left(\zeta'_{1,0}\rho\right)\sin\left(\varphi\right)e^{-\zeta'_{1,0}z}$$

$$= B_0\frac{4}{\pi}\left(q_{m0}/\mu_0\right)R_1\left(\zeta'_{1,0}\rho\right)\sin\left(\varphi\right)e^{-\zeta'_{1,0}(z-z_1)} \tag{372}$$

with

$$R_1\left(\zeta'_{1,n}\rho\right) = J'_1\left(\zeta'_{1,n}a\right)Y_1\left(\zeta'_{1,n}\rho\right) - J_1\left(\zeta'_{1,n}\rho\right)Y'_1\left(\zeta'_{1,n}a\right) \tag{373}$$

Matching to the axial magnetic field at the charge surface

$$H_z\left(\rho,\pi/2,z_1+0\right) = -\frac{\partial\phi_m}{\partial z}\left(\rho,\pi/2,z_1+0\right) = \left(q_{m0}/\mu_0\right)\frac{4}{\pi}\sum_{n=1}^{\infty}A_{+n}\left(j'_{1,n}/b\right)J_1\left(j'_{1,n}\rho/b\right)\ ,\ a<\rho<b$$

$$= 0\ ,\ 0<\rho<a \tag{374}$$

$$H_z\left(\rho,\pi/2,z_1-0\right) = -\frac{\partial\phi_m}{\partial z}\left(\rho,\pi/2,z_1-0\right) = -\left(q_{m0}/\mu_0\right)\frac{4}{\pi}\sum_{n=0}^{\infty}\left(A_{-n}-B_0\delta_{n0}\right)\zeta'_{1,n}R_1\left(\zeta'_{1,n}\rho\right)\ ,\ a<\rho<b \tag{375}$$

The relevant orthogonality relations are

$$\int_a^b R_m\left(\zeta'_{m,n}\rho\right)R_m\left(\zeta'_{m,n'}\rho\right)\rho d\rho = \delta_{nn'}\left[\frac{b^2}{2}\left(1-\frac{m^2}{\zeta'^2_{m,n}b^2}\right)R_m^2\left(\zeta'_{m,n}b\right)-\left(1-\frac{m^2}{\zeta'^2_{m,n}a^2}\right)\frac{2}{\pi^2\zeta'^2_{m,n}}\right] \tag{376}$$

$$\int_0^b J_m\left(j'_{m,n}\rho/b\right)J_m\left(j'_{m,n'}\rho/b\right)\rho d\rho = b^2\int_0^1 J_m\left(j'_{m,n}u\right)J_m\left(j'_{m,n'}u\right)udu = \delta_{nn'}\frac{b^2}{2}\left(1-\frac{m^2}{j'^2_{m,n}}\right)J_m^2\left(j'_{m,n}\right) \tag{377}$$

and thus

$$\int_a^b J_1\left(j'_{1,n}\rho/b\right)H_z\left(\rho,\pi/2,z_1+0\right)\rho d\rho = \left(q_{m0}/\mu_0\right)\frac{4}{\pi}A_{+n}\left(j'_{1,n}/b\right)\frac{b^2}{2}\left(1-\frac{1}{j'^2_{1,n}}\right)J_1^2\left(j'_{1,n}\right)\ ,\ n=1,2,... \tag{378}$$

$$\int_a^b R_1\left(\zeta'_{1,n}\rho\right)H_z\left(\rho,\pi/2,z_1-0\right)\rho d\rho$$

$$= -\left(q_{m0}/\mu_0\right)\frac{4}{\pi}\left(A_{-n}-B_0\delta_{n0}\right)\zeta'_{1,n}\left[\frac{b^2}{2}\left(1-\frac{1}{\zeta'^2_{1,n}b^2}\right)R_1^2\left(\zeta'_{1,n}b\right)-\left(1-\frac{1}{\zeta'^2_{1,n}a^2}\right)\frac{2}{\pi^2\zeta'^2_{1,n}}\right]\ ,\ n=0,1,... \tag{379}$$

Taking the basis

$$\rho H_z\left(\rho,\pi/2,z_1\pm 0\right)=\sum_{j=1}^{J}H_j f_j\left(\rho\right) \tag{380}$$

$$f_j\left(\rho\right)=1\ ,\ \rho_{j-1/2}<\rho<\rho_{j+1/2}$$

$$=0,\text{ otherwise} \tag{381}$$

$$\rho_{1/2}=a \tag{382}$$

$$\rho_{J+1/2}=b \tag{383}$$

$$\rho_j=a+\left(b-a\right)j/J\ ,\ j=0,1,...,J \tag{384}$$

$$\rho_{j+1/2}=\left(\rho_{j+1}+\rho_j\right)/2 \tag{385}$$

gives

$$\int_a^b J_1\left(j'_{1,n}\rho/b\right)H_z\left(\rho,\pi/2,z_1+0\right)\rho d\rho$$

$$=\sum_{j=1}^{J}H_j\int_{\rho_{j-1/2}}^{\rho_{j+1/2}}J_1\left(j'_{1,n}\rho/b\right)d\rho=\sum_{j=1}^{J}\frac{H_j}{j'_{1,n}/b}\left[J_0\left(j'_{1,n}\rho_{j-1/2}/b\right)-J_0\left(j'_{1,n}\rho_{j+1/2}/b\right)\right] \tag{386}$$

$$\int_a^b R_1\left(\zeta'_{1,n}\rho\right)H_z\left(\rho,\pi/2,z_1-0\right)\rho d\rho=\sum_{j=1}^{J}H_j\int_{\rho_{j-1/2}}^{\rho_{j+1/2}}R_1\left(\zeta'_{1,n}\rho\right)d\rho$$

$$=\sum_{j=1}^{J}\frac{H_j}{\zeta'_{1,n}}\left[J'_1\left(\zeta'_{1,n}a\right)\left\{Y_0\left(\zeta'_{1,n}\rho_{j-1/2}\right)-Y_0\left(\zeta'_{1,n}\rho_{j+1/2}\right)\right\}-\left\{J_0\left(\zeta'_{1,n}\rho_{j-1/2}\right)-J_0\left(\zeta'_{1,n}\rho_{j+1/2}\right)\right\}Y'_1\left(\zeta'_{1,n}a\right)\right] \tag{387}$$

Next we match the potential at $z=z_1$

$$B_0R_1\left(\zeta'_{1,0}\rho\right)+\sum_{n=0}^{\infty}A_{-n}R_1\left(\zeta'_{1,n}\rho\right)=\sum_{n=1}^{\infty}A_{+n}J_1\left(j'_{1,n}\rho/b\right)\ ,\ a<\rho<b \tag{388}$$

Inserting the series coefficients

$$\left(\mu_0/q_{m0}\right)\frac{\pi}{4}\int_a^b J_1\left(j'_{1,n}\rho'/b\right)\rho' H_z\left(\rho',\pi/2,z_1+0\right)d\left(\rho'/b\right)=A_{+n}j'_{1,n}\frac{1}{2}\left(1-\frac{1}{j'^2_{1,n}}\right)J_1^2\left(j'_{1,n}\right)\ ,\ n=1,2,... \tag{389}$$

$$\left(\mu_0/q_{m0}\right)\frac{\pi}{4}\int_a^b R_1\left(\zeta'_{1,n}\rho'\right)\rho' H_z\left(\rho',\pi/2,z_1-0\right)d\left(\rho'/b\right)$$

$$= -\left(A_{-n} - B_0\delta_{n0}\right)\zeta'_{1,n}b\left[\frac{1}{2}\left(1-\frac{1}{\zeta'^2_{1,n}b^2}\right)R_1^2\left(\zeta'_{1,n}b\right) - \left(1-\frac{1}{\zeta'^2_{1,n}a^2}\right)\frac{2}{\pi^2\zeta'^2_{1,n}b^2}\right] \ , \ n=0,1,... \qquad (390)$$

then gives the integral equation

$$\frac{4}{\pi}\left(q_{m0}/\mu_0\right)B_0R_1\left(\zeta'_{1,0}\rho\right)$$

$$= \sum_{n=0}^{\infty}\frac{R_1\left(\zeta'_{1,n}\rho\right)}{\zeta'_{1,n}b\left[\left(1-\frac{1}{\zeta'^2_{1,n}b^2}\right)R_1^2\left(\zeta'_{1,n}b\right) - \left(1-\frac{1}{\zeta'^2_{1,n}a^2}\right)\frac{4}{\pi^2\zeta'^2_{1,n}b^2}\right]}\int_a^b R_1\left(\zeta'_{1,n}\rho'\right)\rho' H_z\left(\rho',\pi/2,z_1-0\right)d\left(\rho'/b\right)$$

$$+\sum_{n=1}^{\infty}\frac{J_1\left(j'_{1,n}\rho/b\right)}{j'_{1,n}\left(1-\frac{1}{j'^2_{1,n}}\right)J_1^2\left(j'_{1,n}\right)}\int_a^b J_1\left(j'_{1,n}\rho'/b\right)\rho' H_z\left(\rho',\pi/2,z_1+0\right)d\left(\rho'/b\right) \ , \ a<\rho<b \qquad (391)$$

If we insert the basis expansion

$$\frac{4}{\pi}\left(q_{m0}/\mu_0\right)B_0R_1\left(\zeta'_{1,0}\rho\right)$$

$$= \sum_{n=0}^{\infty}\frac{R_1\left(\zeta'_{1,n}\rho\right)}{\zeta'_{1,n}b\left[\left(1-\frac{1}{\zeta'^2_{1,n}b^2}\right)R_1^2\left(\zeta'_{1,n}b\right) - \left(1-\frac{1}{\zeta'^2_{1,n}a^2}\right)\frac{4}{\pi^2\zeta'^2_{1,n}b^2}\right]}$$

$$\sum_{j=1}^{J}\frac{H_j}{\zeta'_{1,n}b}\left[J'_1\left(\zeta'_{1,n}a\right)\left\{Y_0\left(\zeta'_{1,n}\rho_{j-1/2}\right)-Y_0\left(\zeta'_{1,n}\rho_{j+1/2}\right)\right\} - \left\{J_0\left(\zeta'_{1,n}\rho_{j-1/2}\right)-J_0\left(\zeta'_{1,n}\rho_{j+1/2}\right)\right\}Y'_1\left(\zeta'_{1,n}a\right)\right]$$

$$+\sum_{n=1}^{\infty}\frac{J_1\left(j'_{1,n}\rho/b\right)}{j'_{1,n}\left(1-\frac{1}{j'^2_{1,n}}\right)J_1^2\left(j'_{1,n}\right)}\sum_{j=1}^{J}\frac{H_j}{j'_{1,n}}\left[J_0\left(j'_{1,n}\rho_{j-1/2}/b\right)-J_0\left(j'_{1,n}\rho_{j+1/2}/b\right)\right] \ , \ a<\rho<b \qquad (392)$$

If we integrate against the same basis function to obtain the Galerkin result

$$\frac{4}{\pi}\left(q_{m0}/\mu_0\right)B_0\int_{\rho_{j'-1/2}}^{\rho_{j'+1/2}}R_1\left(\zeta'_{1,0}\rho\right)d\left(\rho/b\right)$$

$$= \sum_{n=0}^{\infty}\frac{1}{\zeta'_{1,n}b\left[\left(1-\frac{1}{\zeta'^2_{1,n}b^2}\right)R_1^2\left(\zeta'_{1,n}b\right) - \left(1-\frac{1}{\zeta'^2_{1,n}a^2}\right)\frac{4}{\pi^2\zeta'^2_{1,n}b^2}\right]}\int_{\rho_{j'-1/2}}^{\rho_{j'+1/2}}R_1\left(\zeta'_{1,n}\rho\right)d\left(\rho/b\right)$$

$$\sum_{j=1}^{J}\frac{H_j}{\zeta'_{1,n}b}\left[J'_1\left(\zeta'_{1,n}a\right)\left\{Y_0\left(\zeta'_{1,n}\rho_{j-1/2}\right)-Y_0\left(\zeta'_{1,n}\rho_{j+1/2}\right)\right\} - \left\{J_0\left(\zeta'_{1,n}\rho_{j-1/2}\right)-J_0\left(\zeta'_{1,n}\rho_{j+1/2}\right)\right\}Y'_1\left(\zeta'_{1,n}a\right)\right]$$

$$+\sum_{n=1}^{\infty}\frac{1}{j'_{1,n}\left(1-\frac{1}{j'^2_{1,n}}\right)J_1^2\left(j'_{1,n}\right)}\int_{\rho_{j'-1/2}}^{\rho_{j'+1/2}}J_1\left(j'_{1,n}\rho/b\right)d\left(\rho/b\right)$$

$$\sum_{j=1}^{J}\frac{H_j}{j'_{1,n}}\left[J_0\left(j'_{1,n}\rho_{j-1/2}/b\right)-J_0\left(j'_{1,n}\rho_{j+1/2}/b\right)\right]\ ,\ j'=1,...,J \tag{393}$$

or

$$\frac{4}{\pi}\left(q_{m0}/\mu_0\right)B_0\frac{1}{\zeta'_{1,0}b}$$

$$\left[J'_1\left(\zeta'_{1,0}a\right)\left\{Y_0\left(\zeta'_{1,0}\rho_{j'-1/2}\right)-Y_0\left(\zeta'_{1,0}\rho_{j'+1/2}\right)\right\}-\left\{J_0\left(\zeta'_{1,0}\rho_{j'-1/2}\right)-J_0\left(\zeta'_{1,0}\rho_{j'+1/2}\right)\right\}Y'_1\left(\zeta'_{1,0}a\right)\right]$$

$$=\sum_{n=0}^{\infty}\frac{1}{\left(\zeta'_{1,n}b\right)^3\left[\left(1-\frac{1}{\zeta'^2_{1,n}b^2}\right)R_1^2\left(\zeta'_{1,n}b\right)-\left(1-\frac{1}{\zeta'^2_{1,n}a^2}\right)\frac{4}{\pi^2\zeta'^2_{1,n}b^2}\right]}$$

$$\left[J'_1\left(\zeta'_{1,n}a\right)\left\{Y_0\left(\zeta'_{1,n}\rho_{j'-1/2}\right)-Y_0\left(\zeta'_{1,n}\rho_{j'+1/2}\right)\right\}-\left\{J_0\left(\zeta'_{1,n}\rho_{j'-1/2}\right)-J_0\left(\zeta'_{1,n}\rho_{j'+1/2}\right)\right\}Y'_1\left(\zeta'_{1,n}a\right)\right]$$

$$\sum_{j=1}^{J}H_j\left[J'_1\left(\zeta'_{1,n}a\right)\left\{Y_0\left(\zeta'_{1,n}\rho_{j-1/2}\right)-Y_0\left(\zeta'_{1,n}\rho_{j+1/2}\right)\right\}-\left\{J_0\left(\zeta'_{1,n}\rho_{j-1/2}\right)-J_0\left(\zeta'_{1,n}\rho_{j+1/2}\right)\right\}Y'_1\left(\zeta'_{1,n}a\right)\right]$$

$$+\sum_{n=1}^{\infty}\frac{1}{j'^3_{1,n}\left(1-\frac{1}{j'^2_{1,n}}\right)J_1^2\left(j'_{1,n}\right)}\left[J_0\left(j'_{1,n}\rho_{j'-1/2}/b\right)-J_0\left(j'_{1,n}\rho_{j'+1/2}/b\right)\right]$$

$$\sum_{j=1}^{J}H_j\left[J_0\left(j'_{1,n}\rho_{j-1/2}/b\right)-J_0\left(j'_{1,n}\rho_{j+1/2}/b\right)\right]\ ,\ j'=1,...,J \tag{394}$$

or

$$\frac{4}{\pi}\left(q_{m0}/\mu_0\right)B_0\frac{1}{\zeta'_{1,0}b}\left[R_1\left(\zeta'_{1,0}\rho_{j'-1/2}\right)-R_1\left(\zeta'_{1,0}\rho_{j'+1/2}\right)\right]$$

$$=\sum_{n=0}^{\infty}\frac{1}{\left(\zeta'_{1,n}b\right)^3\left[\left(1-\frac{1}{\zeta'^2_{1,n}b^2}\right)R_1^2\left(\zeta'_{1,n}b\right)-\left(1-\frac{1}{\zeta'^2_{1,n}a^2}\right)\frac{4}{\pi^2\zeta'^2_{1,n}b^2}\right]}$$

$$\left[R_0\left(\zeta'_{1,0}\rho_{j'-1/2}\right)-R_0\left(\zeta'_{1,0}\rho_{j'+1/2}\right)\right]\sum_{j=1}^{J}H_j\left[R_0\left(\zeta'_{1,0}\rho_{j-1/2}\right)-R_0\left(\zeta'_{1,0}\rho_{j+1/2}\right)\right]$$

$$+\sum_{n=1}^{\infty}\frac{1}{j'^3_{1,n}\left(1-\frac{1}{j'^2_{1,n}}\right)J_1^2\left(j'_{1,n}\right)}\left[J_0\left(j'_{1,n}\rho_{j'-1/2}/b\right)-J_0\left(j'_{1,n}\rho_{j'+1/2}/b\right)\right]$$

$$\sum_{j=1}^{J} H_j \left[J_0\left(j'_{1,n}\rho_{j-1/2}/b\right) - J_0\left(j'_{1,n}\rho_{j+1/2}/b\right)\right] \ , \ j' = 1, ..., J \tag{395}$$

This is a $J \times J$ system we can write as

$$AX = B \tag{396}$$

with elements

$$\frac{4}{\pi}\left(q_{m0}/\mu_0\right) B_0 x_j = H_j \tag{397}$$

$$b_{j'} = \frac{1}{\zeta'_{1,0} b}\left[R_0\left(\zeta'_{1,0}\rho_{j'-1/2}\right) - R_0\left(\zeta'_{1,0}\rho_{j'+1/2}\right)\right] \tag{398}$$

$$a_{j'j} = \sum_{n=0}^{\infty} \frac{1}{\left(\zeta'_{1,n}b\right)^3 \left[\left(1 - \frac{1}{\zeta'^2_{1,n}b^2}\right) R_1^2\left(\zeta'_{1,n}b\right) - \left(1 - \frac{1}{\zeta'^2_{1,n}a^2}\right)\frac{4}{\pi^2\zeta'^2_{1,n}b^2}\right]}$$
$$\left[R_0\left(\zeta'_{1,n}\rho_{j'-1/2}\right) - R_0\left(\zeta'_{1,n}\rho_{j'+1/2}\right)\right]\left[R_0\left(\zeta'_{1,n}\rho_{j-1/2}\right) - R_0\left(\zeta'_{1,n}\rho_{j+1/2}\right)\right]$$

$$+\sum_{n=1}^{\infty} \frac{1}{j'^3_{1,n}\left(1 - \frac{1}{j'^2_{1,n}}\right) J_1^2\left(j'_{1,n}\right)}\left[J_0\left(j'_{1,n}\rho_{j'-1/2}/b\right) - J_0\left(j'_{1,n}\rho_{j'+1/2}/b\right)\right]\left[J_0\left(j'_{1,n}\rho_{j-1/2}/b\right) - J_0\left(j'_{1,n}\rho_{j+1/2}/b\right)\right] \tag{399}$$

and

$$R_1\left(\zeta'_{1,n}\rho\right) = J'_1\left(\zeta'_{1,n}a\right) Y_1\left(\zeta'_{1,n}\rho\right) - J_1\left(\zeta'_{1,n}\rho\right) Y'_1\left(\zeta'_{1,n}a\right) \tag{400}$$

$$R_0\left(\zeta'_{1,n}\rho\right) = J'_1\left(\zeta'_{1,n}a\right) Y_0\left(\zeta'_{1,n}\rho\right) - J_0\left(\zeta'_{1,n}\rho\right) Y'_1\left(\zeta'_{1,n}a\right) \tag{401}$$

From this system solution we then need the coefficients A_{+n}

$$\sum_{j=1}^{J} \frac{H_j}{j'_{1,n}\left(1 - \frac{1}{j'^2_{1,n}}\right) J_1^2\left(j'_{1,n}\right)}\left[J_0\left(j'_{1,n}\rho_{j-1/2}/b\right) - J_0\left(j'_{1,n}\rho_{j+1/2}/b\right)\right] = \left(q_{m0}/\mu_0\right)\frac{2}{\pi} j'_{1,n} A_{+n} \ , \ n = 1, 2, ... \tag{402}$$

or

$$2B_0 \sum_{j=1}^{J} \frac{x_j}{j'_{1,n}\left(1 - \frac{1}{j'^2_{1,n}}\right) J_1^2\left(j'_{1,n}\right)}\left[J_0\left(j'_{1,n}\rho_{j-1/2}/b\right) - J_0\left(j'_{1,n}\rho_{j+1/2}/b\right)\right] = j'_{1,n} A_{+n} \ , \ n = 1, 2, ... \tag{403}$$

In the end we want to determine the tangential magnetic field at the center of the tip of the terminating center conductor of the coax

$$H_y\left(0, z_1 + 0\right) = -\frac{\partial \phi_m}{\partial \rho}\left(0, \pi/2, z_1 + 0\right) = -\left(q_{m0}/\mu_0\right)\frac{4}{\pi}\sum_{n=1}^{\infty}\left(j'_{1,n}/b\right) A_{+n}\left[J'_1\left(j'_{1,n}\rho/b\right)\right]_{\rho\to 0}$$

$$= -\left(q_{m0}/\mu_0\right)\frac{4}{\pi}\sum_{n=1}^{\infty}\left(j'_{1,n}/b\right)A_{+n}\left[J_0\left(j'_{1,n}\rho/b\right)-\frac{1}{j'_{1,n}\rho/b}J_1\left(j'_{1,n}\rho/b\right)\right]_{\rho\to 0}$$

$$= -\left(q_{m0}/\mu_0\right)\frac{2}{\pi}\sum_{n=1}^{\infty}\left(j'_{1,n}/b\right)A_{+n} \tag{404}$$

or

$$H_y\left(0,z_1+0\right)/\left\{4\left(q_{m0}/\mu_0\right)/a\right\}=\frac{a/b}{2\pi}\sum_{n=1}^{\infty}j'_{1,n}A_{+n}$$

$$=\frac{1}{\pi}B_0\left(a/b\right)\sum_{n=1}^{\infty}\sum_{j=1}^{J}\frac{x_j}{j'_{1,n}\left(1-\frac{1}{j'^2_{1,n}}\right)J_1^2\left(j'_{1,n}\right)}\left[J_0\left(j'_{1,n}\rho_{j-1/2}/b\right)-J_0\left(j'_{1,n}\rho_{j+1/2}/b\right)\right] \tag{405}$$

where

$$B_0=\frac{\frac{2}{\zeta'_{1,0}b}R_1\left(\zeta'_{1,0}b\right)}{\left(1-\frac{1}{\zeta'^2_{1,0}b^2}\right)R_1^2\left(\zeta'_{1,0}b\right)-\left(1-\frac{1}{\zeta'^2_{1,0}a^2}\right)\frac{4}{\pi^2\zeta'^2_{1,0}b^2}}e^{-\zeta'_{1,0}z_1} \tag{406}$$

We can write this solution for twice the tip field $2H_y\left(0,z_1+0\right)$ as

$$\left(b/a-1\right)2H_y\left(0,z_1+0\right)e^{\zeta'_{1,0}z_1}/\left\{4\left(q_{m0}/\mu_0\right)/a\right\}=\frac{\left(b/a-1\right)\frac{2}{\pi\zeta'_{1,0}b}R_1\left(\zeta'_{1,0}b\right)}{\left(1-\frac{1}{\zeta'^2_{1,0}b^2}\right)R_1^2\left(\zeta'_{1,0}b\right)-\left(1-\frac{1}{\zeta'^2_{1,0}a^2}\right)\frac{4}{\pi^2\zeta'^2_{1,0}b^2}}$$

$$2\left(a/b\right)\sum_{n=1}^{\infty}\sum_{j=1}^{J}\frac{x_j}{j'_{1,n}\left(1-\frac{1}{j'^2_{1,n}}\right)J_1^2\left(j'_{1,n}\right)}\left[J_0\left(j'_{1,n}\rho_{j-1/2}/b\right)-J_0\left(j'_{1,n}\rho_{j+1/2}/b\right)\right]$$

$$=\left[\left(b/a-1\right)H_\varphi^{LM}\left(a,0,z_1\right)e^{\zeta'_{1,0}z_1}/\left\{4\left(q_{m0}/\mu_0\right)/a\right\}\right]$$

$$\frac{2}{\left(\frac{b}{a}\right)^2\left(\frac{2}{\pi\zeta'_{1,0}b}\right)}\sum_{n=1}^{\infty}\sum_{j=1}^{J}\frac{x_j}{j'_{1,n}\left(1-\frac{1}{j'^2_{1,n}}\right)J_1^2\left(j'_{1,n}\right)}\left[J_0\left(j'_{1,n}\rho_{j-1/2}/b\right)-J_0\left(j'_{1,n}\rho_{j+1/2}/b\right)\right] \tag{407}$$

where the approximation using the lowest mode in the coax is

$$\left(b/a-1\right)H_\varphi^{LM}\left(a,0,z_1\right)e^{\zeta'_{1,0}z_1}/\left\{4\left(q_{m0}/\mu_0\right)/a\right\}\approx\frac{\left(b/a-1\right)\left(b/a\right)\left(\frac{2}{\pi\zeta'_{1,0}b}\right)^2R_1\left(\zeta'_{1,0}b\right)}{\left(1-\frac{1}{\zeta'^2_{1,0}b^2}\right)R_1^2\left(\zeta'_{1,0}b\right)-\left(1-\frac{1}{\zeta'^2_{1,0}a^2}\right)\left(\frac{2}{\pi\zeta'_{1,0}b}\right)^2} \tag{408}$$

Figure 5 shows this numerical solution (407) with $J=100$ as the black curve; the dashed gray curve is the preceding lowest order mode result (408) and the light gray curve is the ratio of the black and dashed gray curve (correction to lowest order mode result). A fit is given by

$$\left(b/a-1\right)H_\varphi^{LM}\left(a,0,z_1\right)e^{\zeta'_{1,0}z_1}/\left\{4\left(q_{m0}/\mu_0\right)/a\right\}\approx 0.4+0.65\left(a/b\right)^2+0.15\left(a/b\right)^6 \tag{409}$$

which is shown as the dash-dot curve.

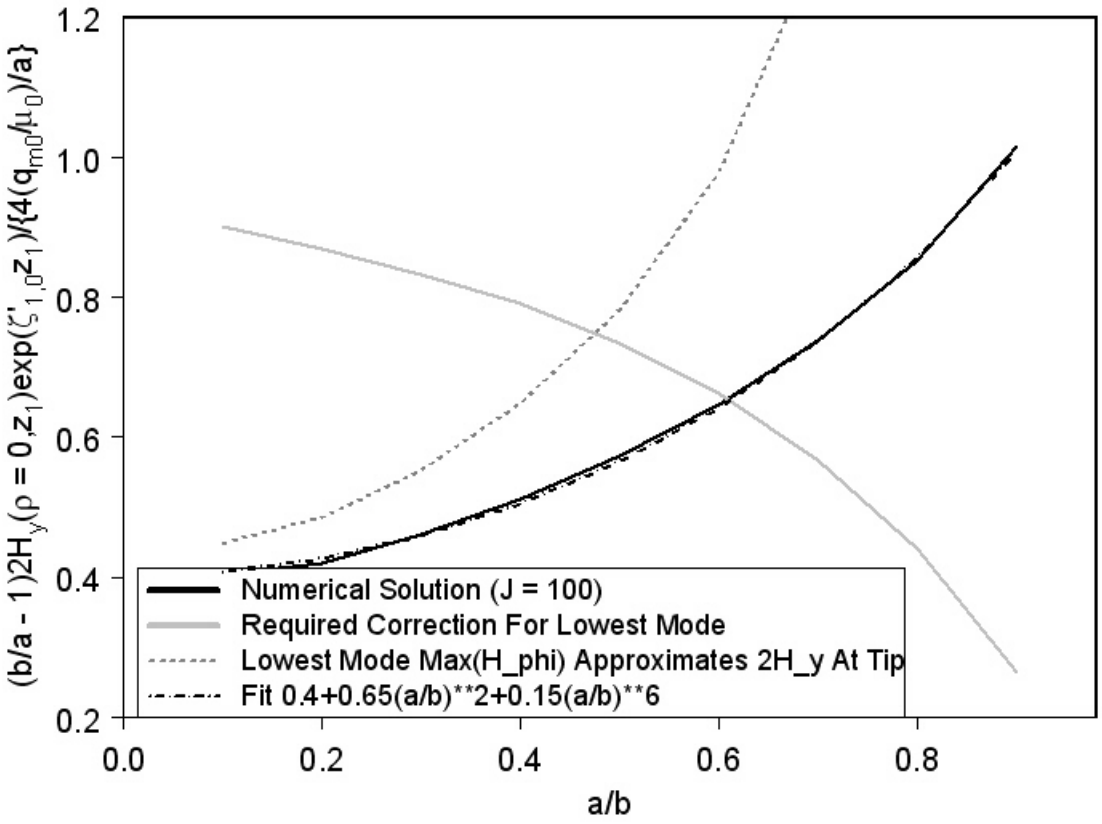

Figure 5: The solid black curve is the maximum magnetic field (current density) at the center of the tip of the terminating center conductor as a function of the ratio of inner-to-outer coaxial radii. The dash-dot curve is a simple fit. The gray dashed curve is the approximation discussed in the prior section, using the maximum magnetic field of the dominant coaxial mode around a continuing coax at the location of the actual termination (the solid gray curve is the ratio of the black to gray dashed curves).

4.6 Cap To Connector Inductance/Resistance And Pin Voltage

We can apply the preceding current density driven by the magnetic field to the preceding formulas for the connector cap inductance [1]

$$V_{\max} = V_{\max}^{ext} + V_{\max}^{int} \tag{410}$$

with external inductive cap voltage

$$V_{\max}^{ext} = L_{\max}^{cap} 2h_{cap} \frac{d}{dt} K_{sc}^{cap} \leq L_{\max}^{cap} 2h_{cap} K_{sc}^{cap} / \tau_r \tag{411}$$

and internal cap voltage

$$\frac{1}{2} V_{\max}^{int} = \frac{L_{\max}}{\mu_0 w_{cap}} \sqrt{\mu/\sigma} \frac{d^{1/2}}{dt^{1/2}} I_{pin} \leq \sqrt{\frac{4\mu t}{\pi\sigma}} \frac{L_{\max}}{\mu_0 w_{cap}} I_{pin}/\tau_r$$

$$= \frac{L_{\max}}{\mu_0 w_{cap}} \sqrt{\mu/\sigma} 2h_{cap} \frac{d^{1/2}}{dt^{1/2}} K_{sc}^{cap} \leq \sqrt{\frac{4\mu t}{\pi\sigma}} \frac{L_{\max}}{\mu_0 w_{cap}} 2h_{cap} K_{sc}^{cap} / \tau_r \tag{412}$$

with maximum in time

$$\frac{1}{2} V_{\max}^{int} \leq \sqrt{\frac{4\mu\tau_r}{\pi\sigma}} \frac{L_{\max}^{cap}}{\mu_0 w_{cap}} 2h_{cap} K_{sc}^{cap} / \tau_r \tag{413}$$

There is also an internal voltage contribution due to the pin itself (between cap and connector base). If the current is confined to the surface of the pin for the rise time region

$$V_{pin}^{int} = \frac{w_{cap}}{2\pi a_{pin}} \sqrt{\mu_p/\sigma_p} \frac{\partial^{1/2}}{\partial t^{1/2}} I_{pin}(t) = \frac{w_{cap}}{2\pi a_{pin}} \sqrt{\frac{4\mu_p t}{\pi\sigma_p}} (I_{pin}/\tau_r) \tag{414}$$

with maximum value

$$V_{pin}^{int} \leq \frac{w_{cap}}{2\pi a_{pin}} \sqrt{\frac{4\mu_p \tau_r}{\pi\sigma_p}} (I_{pin}/\tau_r) \tag{415}$$

where μ_p and σ_p are the magnetic permeability and conductivity of the pin material. Therefore

$$V_{\max} \leq \left[L_{\max}^{cap} \left(1 + \sqrt{\frac{4\mu\tau_r}{\pi\sigma}} \frac{2}{\mu_0 w_{cap}} \right) + \frac{w_{cap}}{2\pi a_{pin}} \sqrt{\frac{4\mu_p \tau_r}{\pi\sigma_p}} \right] 2h_{cap} K_{sc}^{cap} / \tau_r \tag{416}$$

The estimate for this cap inductance due to the cap-to-connector base slots [1], [6] is

$$L_{\max}^{cap} \sim \frac{\mu_0 w_{cap}}{2\pi} \ln\left(\frac{h_{cap}}{\pi a_{pin}} \right) \ , \ d_{cap} >> \ell_{cap} = 2h_{cap} \tag{417}$$

or

$$L_{\max}^{cap} \sim \frac{1}{4} \mu_0 h_{cap} \frac{w_{cap}}{d_{cap}} + \frac{\mu_0 w_{cap}}{2\pi} \ln\left[\frac{d_{cap}/(2\pi a_{pin})}{\cos(\pi f_{pin}/d_{cap})} \right] \ , \ d_{cap} << \ell_{cap} \tag{418}$$

where $2h_{cap} = \ell_{cap}$ is the distance between pin contacts, d_{cap} is the overlap depth, w_{cap} is the gap width, a_{pin} is the pin radius, and f_{pin} is the displacement of the pins from the depth center toward the interior of

the connector. For $f_{pin} = 0$ a function which incorporates both these limits, and remains uniformly valid, is [1]

$$L_{\max}^{cap} \approx \frac{1}{4}\mu_0 h_{cap}\frac{w_{cap}}{d_{cap}} + \frac{\mu_0 w_{cap}}{2\pi}\left[\ln\left(\frac{d_{cap}/2}{h_{cap}+d_{cap}/2}\right) - \ln\left(1-e^{-\pi a_{pin}/h_{cap}}\right)\right] \ , \ f_{pin} = 0 \tag{419}$$

Near the outer radius of the cap, but interior to the connector, the voltage appears at the top of the cap, where the cap insulator exists. This voltage spreads out to develop the electric field near the pins. We estimate the electric field at the pins by using the a parallel plate formula

$$h_{conn}E_{cap} \sim V_{\max}^{cap} \tag{420}$$

where h_{conn} is the height of the cap above the base of the pins. If the insulator is foam with a dielectric constant near unity, the height h_{conn} is the distance to the cap metallic surface. Alternatively, if it is a solid dielectric this height should be reduced somewhat (the thickness of the insulator reduced by the inverse of the dielectric constant) to account for the dielectric constant of the insulator.

5 OTHER PENETRATION MECHANISMS

If the cylindrical barrier has any small holes (circular hole results are given here) we can estimate interior fields by estimating the hole dipole moments either for a direct lightning strike or the fields from a close strike. Another mechanism is direct diffusion of the low frequency lightning field through the conductive barrier; although uniform field drives can be easily treated, the practical worst case drive is a strike to some exterior conductor near the barrier surface, providing a line source current drive.

5.1 Hole Fields

If there is a small circular hole in the outer cylindrical shield, we can estimate the penetrant magnetic and electric fields. The magnetic field through an open hole in a thin shield is large but decreases rapidly with distance, and the thickness of the shield causes exponential decay of the penetrant amplitude. Let us use the magnetic dipole moment of a circular hole to see how big the magnetic field at a distance will be. In this section we define the dipole moments taking into account the presence of the ground plane (in other words the potential and fields can be found in free space from these moments). The dipole moment for a wire (carrying lightning current) laying across a circular aperture of radius a_{hole} is [2]

$$m_y = -2I_0\left(t\right)a_{hole}^2 \tag{421}$$

If we had an excitation of a uniform short circuit field H_y^{sc} instead of this localized source, the general definition of the aperture magnetic dipole moment in terms of the magnetic polarizability $\alpha_m = \alpha_{m,yy}$ is [8]

$$m_y = -2\alpha_m H_y^{sc} \tag{422}$$

where in a thin shield the polarizability is [8]

$$\alpha_m^0 = \frac{4}{3}a_{hole}^3 \tag{423}$$

The shield in this case often has a large wall thickness Δ, and thus the polarizability for this case is modified to [9]

$$\alpha_m \approx \alpha_m^0\, 0.838\, e^{-j_{11}'(\Delta/a_{hole})} \tag{424}$$

where $j_{11}' = 1.841$ is the first root of $J_1'\left(x\right) = 0$. In our case with the local current excitation we thus include the exponential decay factor

$$m_y \approx -2I_0\left(t\right)a_{hole}^2 e^{-j_{11}'(\Delta/a_{hole})} \tag{425}$$

The magnetic potential from this dipole moment is then

$$\phi_m = \frac{\underline{m}\cdot\underline{r}}{4\pi r^3} = \frac{m_y \sin\theta\sin\varphi}{4\pi r^2} \tag{426}$$

The magnetic field is then

$$\underline{H} = -\nabla\phi_m \tag{427}$$

or

$$H_r = -\frac{\partial}{\partial r}\phi_m = \frac{m_y\sin\theta\sin\varphi}{2\pi r^3} = -\frac{I_0\left(t\right)\left(a_{hole}/r\right)^2\sin\theta\sin\varphi}{\pi r}e^{-j_{11}'(\Delta/a_{hole})} \tag{428}$$

$$H_\theta = -\frac{1}{r}\frac{\partial}{\partial\theta}\phi_m = -\frac{m_y \cos\theta \sin\varphi}{4\pi r^3} = \frac{I_0\left(t\right)\left(a_{hole}/r\right)^2 \cos\theta \sin\varphi}{2\pi r} e^{-j'_{11}(\Delta/a_{hole})} \tag{429}$$

$$H_\varphi = -\frac{1}{r\sin\theta}\frac{\partial}{\partial\varphi}\phi_m = -\frac{m_y \cos\varphi}{4\pi r^3} = \frac{I_0\left(t\right)\left(a_{hole}/r\right)^2 \cos\varphi}{2\pi r} e^{-j'_{11}(\Delta/a_{hole})} \tag{430}$$

The field values can double on an interior conductor surface. Hole depth (waveguide decay) reduces these levels if the wall thickness is substantial. Skin depth can effectively increase the hole radius, but we are interested in the time derivative of the magnetic field, so the early time $t = \tau_r$, is of primary interest.

There is also an electric dipole moment of the hole, which for a uniform drive field E_z^{sc} is [8]

$$p_z = 2\varepsilon_0 \alpha_e E_z^{sc} \tag{431}$$

and for a circular hole the polarizability in a thin screen is [8]

$$\alpha_e^0 = \frac{2}{3} a_{hole}^3 \tag{432}$$

For a large thickness this is modified to [9]

$$\alpha_e \approx \alpha_e^0\, 0.825 e^{-j_{0,1}(\Delta/a_{hole})} \tag{433}$$

where $j_{0,1} = 2.405$ is the first root of $J_0\left(x\right) = 0$. In our case we simply add the exponential decay

$$p_z \approx 2\varepsilon_0 \frac{2}{3} a_{hole}^3 E_z^{sc}\left(t\right) e^{-j_{0,1}(\Delta/a_{hole})} \tag{434}$$

The electric potential from this electric dipole moment is then

$$\phi = \frac{\underline{p}\cdot\underline{r}}{4\pi\varepsilon_0 r^3} = \frac{p_z \cos\theta}{4\pi\varepsilon_0 r^2} \tag{435}$$

The electric field is then

$$\underline{E} = -\nabla\phi \tag{436}$$

or

$$E_r = -\frac{\partial}{\partial r}\phi = \frac{p_z \cos\theta}{2\pi\varepsilon_0 r^3} = \frac{2}{3\pi}\left(a_{hole}/r\right)^3 E_z^{sc}\left(t\right) e^{-j_{0,1}(\Delta/a_{hole})} \cos\theta \tag{437}$$

$$E_\theta = -\frac{1}{r}\frac{\partial}{\partial\theta}\phi = -\frac{p_z \sin\theta}{4\pi\varepsilon_0 r^3} = -\frac{1}{3\pi}\left(a_{hole}/r\right)^3 E_z^{sc}\left(t\right) e^{-j_{0,1}(\Delta/a_{hole})} \sin\theta \tag{438}$$

$$E_\varphi = 0 \tag{439}$$

We take the planar breakdown level for the electric field to be the typical 3 MV/m or

$$E_z^{sc} \leq 30 \text{ kV/cm} \tag{440}$$

with a time rate of change of roughly τ_r.

5.1.1 Hole Cover

If a hole cover is in place, made out of anodized aluminum, then there will be a thin slot around the cover instead of an open hole. The slot can behave in a similar manner to the door slot, except it is taken to be much smaller in overall diameter. The magnetic charge per unit length around the slot $q_m(s)$ will generate the magnetic dipole moment in this case $h_{hole} = \pi a_{hole}$

$$\underline{m} = \frac{1}{\mu_0}\int_{-h_{hole}}^{h_{hole}} q_m(s)\,\underline{r}\,ds \tag{441}$$

$$\frac{1}{2}q_m(s) = L_{anod}\frac{1}{2}I_0(t)\,\mathrm{sgn}(s) \tag{442}$$

$$\frac{1}{2}m_y = \frac{1}{\mu_0}L_{anod}I_0(t)\,a_{hole}^2\int_0^{\pi}\sin\varphi d\varphi = (L_{anod}/\mu_0)\,I_0(t)\,2\pi a_{hole}^2 \tag{443}$$

$$L_{anode}/\mu_0 = \pi/\Omega_e^{hole} \tag{444}$$

$$\Omega_e^{hole} \approx 2\ln(8h_{hole}/w_{hole}) + \pi d_{hole}/w_{hole} \tag{445}$$

When Ω_e^{hole} is large, this dipole moment is much smaller then the open hole dipole moment of the preceding section. Skin effect can increase the effective hole radius here. If the hole depth $d_{hole} > h_{hole}$ there will be exponential decay in this slot gap region. Instead we add the preceding exponential decay through the hole

$$m_y = 2\,(L_{anod}/\mu_0)\,I_0(t)\,2\pi a_{hole}^2 e^{-j'_{11}(\Delta/a_{hole})} \tag{446}$$

and thus

$$H \approx \frac{2I_0(t)/r}{(2/\pi)\ln(8h_{hole}/w_{hole}) + d_{hole}/w_{hole}}\,(a_{hole}/r)^2\,e^{-j'_{11}(\Delta/a_{hole})} \tag{447}$$

The electric dipole moment of the hole is now created by the voltage of the cover and is reduced from the open hole case.

$$p_z = -\frac{1}{2}\varepsilon_0 a_{hole}\int_{-h_{hole}}^{h_{hole}} I_m(s)\,ds = -\frac{1}{2}\varepsilon_0\langle I_m\rangle\,\pi a_{hole}^2 \tag{448}$$

where the magnetic current of the gap is taken as

$$I_m(s) = 2V(s) \tag{449}$$

Adding the exponential decay factor

$$p_z \approx -\frac{1}{2}\varepsilon_0\langle I_m\rangle\,\pi a_{hole}^2 e^{-j_{0,1}(\Delta/a_{hole})} \tag{450}$$

After breakdown of the cover at a point, the voltage assumes a linear profile around the azimuth, and thus

$$\langle I_m(s)\rangle = 2\langle V(s)\rangle = V(0) \tag{451}$$

with

$$V(0) = \frac{1}{2}(I_0/\tau_r)\,h_{hole}L_{anod} \tag{452}$$

and

$$E \approx \frac{\mu_0 h_{hole} \left(I_0/\tau_r \right) / \left(8r \right)}{(2/\pi) \ln \left(8h_{hole}/w_{hole} \right) + d_{hole}/w_{hole}} \left(a_{hole}/r \right)^2 e^{-j_{0,1}(\Delta/a_{hole})} \tag{453}$$

Also, because breakdown is now a possible mechanism for initial contact of the cover with the surrounding enclosure, there can be an initial increase in the change of the electric dipole moment with time, and the collapse from a uniform voltage gives

$$\langle I_m \left(s \right) \rangle = 2 \langle V \left(s \right) \rangle = 2V_0 \tag{454}$$

and therefore

$$E \approx \frac{V_0}{2r} \left(a_{hole}/r \right)^2 e^{-j_{0,1}(\Delta/a_{hole})} \tag{455}$$

Experimental evidence gives $V_0 \leq 1$ kV [10] and a breakdown time of $O\left(1 \text{ ns}\right)$. This electric field limit also overrides the preceding result driven by the lightning current.

5.2 Diffusion Field

We now summarize the diffusion penetration. The cylindrical wall has thickness Δ. To treat this problem we give the field penetration through a conductive layer with conductivity σ driven by a decaying electric line current exterior to the barrier

$$I \left(t \right) = I_0 e^{-\alpha t} \ , \ I_0 = 200 \text{ kA}, \ \alpha = 1/ \left(288 \ \mu \text{s} \right) \tag{456}$$

modeled by a transfer impedance boundary condition. This simplified boundary condition usually gives accurate results for the distance between source and observation point ρ_0 larger than the wall thickness Δ

$$H_x \left(0, \rho_0 \right) = -\frac{I_0}{2\pi s_i} \left[-\frac{e^{-\alpha t}}{\rho_0/s_i} + \frac{1}{\alpha t + \rho_0/s_i} + e^{-\alpha t - \rho_0/s_i} \left\{ \text{Ei} \left(\rho_0/s_i \right) - \text{Ei} \left(\alpha t + \rho_0/s_i \right) \right\} \right] \ , \ \rho_0 > \Delta \tag{457}$$

where the electrical distance associated with the transfer impedance boundary condition is ($\mu_0 = 4\pi \times 10^{-7}$ H/m)

$$s_i = 1/ \left(\alpha \mu_0 \sigma \Delta / 2 \right) \tag{458}$$

and we have frequently used the electrical conductivity of 304 stainless steel alloy $\sigma = 1.4 \times 10^6$ S/m or commercial aluminum 6061 alloy with $\sigma = 2.6 \times 10^6$ S/m. The exponential integral is defined as the principal value integral

$$\text{Ei} \left(x \right) = -PV \int_{-x}^{\infty} e^{-u} \frac{du}{u} \tag{459}$$

For $\rho_0 >> s_i$ we can use the asymptotic expansion

$$\text{Ei} \left(x \right) \sim \left(e^x/x \right) \left[1 + 1/x + ... + n!/x^n + ... \right] \ , \ x >> 1 \tag{460}$$

to rewrite this field as

$$H_x \sim \frac{I_0}{2\pi \rho_0} \left[-\frac{e^{-\alpha t}}{\rho_0/s_i} + \frac{\rho_0/s_i}{\left(\alpha t + \rho_0/s_i \right)^2} \right] \ , \rho_0 >> s_i, \rho_0 > \Delta \tag{461}$$

Taking the time derivative

$$\frac{\partial}{\partial t}H_x \sim \frac{I_0}{2\pi\rho_0}\left[\frac{\alpha e^{-\alpha t}}{\rho_0/s_i} - \frac{2\alpha\rho_0/s_i}{\left(\alpha t+\rho_0/s_i\right)^3}\right] \ , \rho_0 >> s_i, \rho_0 > \Delta \tag{462}$$

and setting $\alpha t << 1$

$$\frac{\partial}{\partial t}H_x \sim \frac{I_0\alpha s_i}{2\pi\rho_0^2} = \frac{I_0}{\pi\rho_0^2\mu_0\sigma\Delta} \ , \rho_0 >> s_i, \rho_0 > \Delta \tag{463}$$

If we have several different conductive layers we can use the total thickness

$$\Delta = \sum_{j=1}^{J}\Delta_j \tag{464}$$

and effective conductivity σ_e

$$\Delta/\sigma_e = \sum_{j=1}^{J}\Delta_j/\sigma_j \tag{465}$$

We then use

$$s_i = 1/\left(\alpha\mu_0\sigma_e\Delta/2\right) \tag{466}$$

and

$$\frac{\partial}{\partial t}H_x \sim \frac{I_0\alpha s_i}{2\pi\rho_0^2} = \frac{I_0}{\pi\rho_0^2\mu_0\sigma_e\Delta} \ , \rho_0 >> s_i, \rho_0 > \Delta \tag{467}$$

The electric field from diffusion is small since it is created by current flow through the surface impedance of the metallic wall.

This page left blank

6 CONCLUSIONS

This report considers a cylindrical enclosure, with a door at one end having a circular or azimuthal slot penetration, when struck by lightning. Interior to the enclosure is a coaxial structure topology having an open circuit at the opposite end with a capped connector. Using approximate analytical techniques the penetration of the drive fields and final coupling to the connector pins is estimated.

The report provides formulas for the average door voltage (26), plus hinge voltage (35), when struck by lightning. The induced center conductor coaxial voltage is (263), with capacitances (262), (260), and voltage drive (255). The resulting interior center conductor electric field (159) is determined, along with approximate values (181) and (182). These are used to find the connector cap short circuit current (200), connector cap voltage (211), and finally the pin voltage (216); because of the high impedance associated with the Thevinen equivalent circuit at the low frequencies associated with lightning we expect the voltage delivered to a load to be further reduced (221).

The magnetic field drive to the connector is also treated. The door slot charge per unit length (315), drives the dominant mode magnetic potential (334), with decay constant (336). The tip magnetic field (407) and (409), or approximate value from the dominant coaxial mode (408), drives the connector cap and gives voltage (416).

The low frequency coaxial modes are examined in some detail with approximations given to estimate capacitance and fields at terminated ends through closed form fits shown in the Figures.

The reduction in the door voltage drive when a conductive gasket in the door slot is used is given by (65). The reduction in magnetic field drive when a conductive gasket in the door slot is used is given by (364), which is nearly the same as the voltage reduction due to the gasket.

The field penetration through a small circular hole in the wall is given for the magnetic field by (428) and for the electric field by (437). The penetration through a circular hole with cover is given for the magnetic field by (447) and for the electric field by (453).

The diffusion penetration mechanism produces an interior magnetic field derivative (467) when driven by an exterior line source lightning current.

References

[1] L. K. Warne, W. A. Johnson, K. C. Chen, and K. O. Merewether, "Joint Voltages Resulting From Lightning Currents," SAND2007-1267, March 2007.

[2] R. E. Jorgenson and L. K. Warne, "Useful Equations For Calculating The Induced Voltage Inside A Faraday Cage That Has Been Struck By Lightning," SAND2001-2950, Sept. 2001.

[3] S. Ramo, J. R. Whinnery, and R. Van Duzer, **Fields And Waves In Communication Electronics**, New York: John Wiley & Sons, Inc., 1965, pp. 311-313.

[4] M. Abramowitz and I. A. Stegun (editors), Handbook of Mathematical Functions, National Bureau of Standards, Dec. 1972, pp. 299, 371, 374, 409, 415.

[5] L. K. Warne, L. I. Basilio, W. A. Johnson, M. E. Morris, M. B. Higgins, and J. M. Lehr, "Capacitance and Effective Area of Flush Mounted Monopole Probes," SAND2004-3994, Sept. 2004.

[6] L. K. Warne, W. A. Johnson, B. F. Zinser, W. L. Langston, R. S. Coats, I. C. Reines, J. T. Williams, L. I. Basilio, and K. C. Chen, "Narrow Slot Algorithm," SAND2020-3979, April 2020.

[7] L. K. Warne, W. A. Johnson, L. I. Basilio, W. L. Langston, and M. B. Sinclair, "Subcell Method For Modeling Metallic Resonators In Metamaterials," PIER B, Vol. 38, pp. 135-164, 2012.

[8] K. S. H. Lee (editor), **EMP Interaction: Principles, Techniques, and Reference Data**, New York: Hemisphere Pub. Corp., 1986, p. 441.

[9] L. K. Warne, L. I. Basilio, W. L. Langston, K. C. Chen, H. G. Hudson, M. E. Morris, S. L. Stronach, W. A. Johnson, and W. Derr, "Electromagnetic Coupling Into Two Standard Calibration Shields On The Sandia Cable Tester," Sandia National Laboratories Report, SAND2014-0842, February 2014.

[10] M. A. Dinallo and R. J. Fisher, "Voltages Across Assembly Joints Due To Direct-Strike Lightning Currents," Sandia National Laboratories Report, SAND93-0788, August 1994.

DISTRIBUTION

Email—Internal

Name	Org.	Sandia Email Address
K. O. Merewether	02900	MS0405
W. L. Langston	01324	MS1152
J. D. Kotulski	01324	MS1152
A. R. Pack	01322	MS1152
R. A. Pfeiffer	01324	MS1152
L. San Martin	01322	MS1152
L. K. Warne	01324	MS1152
Technical Library	01911	sanddocs@sandia.gov

Hardcopy—Internal

Number of Copies	Name	Org.	Mailstop
2	L. San Martin	01322	MS1152
2	L. K. Warne	01324	MS1152

Sandia National Laboratories

Sandia National Laboratories is a multimission laboratory managed and operated by National Technology & Engineering Solutions of Sandia LLC, a wholly owned subsidiary of Honeywell International Inc. for the U.S. Department of Energy's National Nuclear Security Administration under contract DE-NA0003525.